

Provided for non-commercial research and education use.
Not for reproduction, distribution or commercial use.



This article appeared in a journal published by Elsevier. The attached copy is furnished to the author for internal non-commercial research and education use, including for instruction at the authors institution and sharing with colleagues.

Other uses, including reproduction and distribution, or selling or licensing copies, or posting to personal, institutional or third party websites are prohibited.

In most cases authors are permitted to post their version of the article (e.g. in Word or Tex form) to their personal website or institutional repository. Authors requiring further information regarding Elsevier's archiving and manuscript policies are encouraged to visit:

<http://www.elsevier.com/copyright>



Contents lists available at ScienceDirect

Journal of Human Evolution

journal homepage: www.elsevier.com/locate/jhevol

The dating and interpretation of a Mode 1 site in the Luangwa Valley, Zambia

Lawrence Barham^{a,*}, William M. Phillips^{b,1}, Barbara A. Maher^c, Vassil Karloukovski^c, Geoff A.T. Duller^d, Mayank Jain^e, Ann G. Wintle^d^a School of Archaeology, Classics and Egyptology, University of Liverpool, Hartley Building, Liverpool L69 3GS, UK^b Institute of Geography, University of Edinburgh, Edinburgh EH8 9XP, UK^c Centre for Environmental Magnetism and Palaeomagnetism, Lancaster Environment Centre, University of Lancaster, Bailrigg, Lancaster, LA1 4YQ, UK^d Institute of Geography and Earth Sciences, Aberystwyth University, Ceredigion SY23 3DB, UK^e Radiation Research Division, Risø National Laboratory for Sustainable Energy, Technical University of Denmark, DK-4000, Denmark

ARTICLE INFO

Article history:

Received 15 May 2009

Accepted 4 October 2010

Keywords:

South-central Africa

Cosmogenic nuclide dating

Palaeomagnetism

Isothermal thermoluminescence

ABSTRACT

Flake based assemblages (Mode 1) comprise the earliest stone technologies known, with well-dated Oldowan sites occurring in eastern Africa between ~ 2.6–1.7 Ma, and in less securely dated contexts in central, southern and northern Africa. Our understanding of the spread and local development of this technology outside East Africa remains hampered by the lack of reliable numerical dating techniques applicable to non-volcanic deposits. This study applied the still relatively new technique of cosmogenic nuclide burial dating (¹⁰Be/²⁶Al) to calculate burial ages for fluvial gravels containing Mode 1 artefacts in the Luangwa Valley, Zambia. The Manzi River, a tributary of the Luangwa River, has exposed a 4.7 m deep section of fluvial sands with discontinuous but stratified gravel layers bearing Mode 1, possibly Oldowan, artefacts in the basal layers. An unconformity divides the Manzi section, separating Mode 1 deposits from overlying gravels containing Mode 3 (Middle Stone Age) artefacts. No diagnostic Mode 2 (Acheulean) artefacts were found.

Cosmogenic nuclide burial dating was attempted for the basal gravels as well as exposure ages for the upper Mode 3 gravels, but was unsuccessful. The complex depositional history of the site prevented the calculation of reliable age models. A relative chronology for the full Manzi sequence was constructed, however, from the magnetostratigraphy of the deposit (N>R>N sequence). Isothermal thermoluminescence (ITL) dating of the upper Mode 3 layers also provided consistent results (~ 78 ka). A coarse but chronologically coherent sequence now exists for the Manzi section with the unconformity separating probable mid- or early Pleistocene deposits below from late Pleistocene deposits above. The results suggest Mode 1 technology in the Luangwa Valley may post-date the Oldowan in eastern and southern Africa. The dating programme has contributed to a clearer understanding of the geomorphological processes that have shaped the valley and structured its archaeological record.

© 2010 Elsevier Ltd. All rights reserved.

Introduction

The development of potassium–argon dating in the early 1960s and its application to deeply stratified East Africa Rift Valley sedimentary sequences has transformed not only the chronology of the earliest archaeological record but also our understanding of its broader evolutionary contexts (Plummer, 2004). Recent refinements in single crystal Ar/Ar dating have improved the accuracy and precision of dating volcanic deposits that act as local and regional marker horizons across tectonic basins (e.g., Gathogo and

Brown, 2006). As a result, palaeoanthropologists are now able to develop and test holistic models of hominin behavioural and biological responses to differing scales of ecological change (e.g., Potts, 2001). Such complex modelling would have been unthinkable pre-1960s, but for much of the African record outside the tectonically active Rift Valley such fine-grained chronological frameworks remain elusive. There are few numerical dating techniques currently available that span the Miocene to Pleistocene and which can be applied to the fluvial and lacustrine contexts which attracted hominin occupation and contain their archaeological and fossil

* Corresponding author.

E-mail address: l.s.barham@liv.ac.uk (L. Barham).¹ Current address: Idaho Geological Survey, University of Idaho, Moscow ID 83844-3014, USA

remains. As a result, East African Rift basin sequences retain their position as key references for inter-regional chronology building across the continent. Long distance biostratigraphic correlations with the East African record, often underpinned by magnetic polarity records, continue to be used by palaeoanthropologists working in northern Africa (Sahnouni et al., 2002), and this is a recognised although problematic strategy for the relative dating of the South African karstic caves and river terrace sequences (Partridge, 2000; Williams et al., 2007). The application of numerical dating techniques, notably uranium-series (U–Pb) and cosmogenic nuclide burial dating using ^{26}Al and ^{10}Be , to cave sediments promises independent chronological controls for biostratigraphic sequences, but as in the case of Sterkfontein (Member 2) the results vary greatly between techniques, with U–Pb indicating a considerably younger age (~ 2.2 Ma) for the deposit than that suggested by cosmogenic dating (~ 4 Ma; Partridge et al., 2003; Walker et al., 2006). The marked discrepancy in results highlights the importance of crosschecking results against other methodologically independent methods of dating. More recently, a single cosmogenic nuclide burial age of ~ 2 Ma has been reported from the site of Wonderwerk Cave (South Africa) and supports the interpretation of the palaeomagnetic record associated with a Mode 1 assemblage (Chazan et al., 2008:8). An early Pleistocene cosmogenic nuclide burial age of ca. 1.6 Ma has also been obtained from deep fluvial deposits containing Mode 2 (Acheulean) artefacts from the Vaal River terraces, South Africa (Gibbon et al., 2009). These cosmogenic results accord with radiometric and biostratigraphic time ranges for the Oldowan and Acheulean in eastern and southern Africa, supporting models of a widespread transmission of these technologies in the early Pleistocene (Barham and Mitchell, 2008). In the Chad Basin, dating using atmospheric ^{10}Be has now provided the first radiometric dates from the shallow deposits containing Miocene *Sahelanthropus tchadensis* (6.8–7.2 Ma) and Pliocene *Australopithecus bahrelghazali* (~ 3.58 Ma; Lebatard et al., 2008). The dating results match closely initial age estimates based on long-distance faunal correlations with the East African record (Brunet et al., 1995, 2002). Cosmogenic nuclide burial dating is still, from a palaeoanthropological perspective, in an early stage of development and in need of further testing through application to build confidence in its reliability before it can be used as a stand-alone technique.

We report here on the application of cosmogenic nuclide dating to determine the burial age of fluvial deposits containing Early Stone Age artefacts (Mode 1) but which lack associated fauna for making biostratigraphic correlations. The fluvial deposits occur in the Luangwa Valley, eastern Zambia, and the largely acidic sediments and ground water make bone preservation a rarity, though with some notable exceptions (Elton et al., 2003; Bishop, in prep). High natural background radiation in the Luangwa sediments also limits the age range for optically stimulated luminescence dating to less than 200 ka (see below). These unpromising circumstances would normally limit the chronological resolution to one of a relative sequence based on typological comparisons with numerical dated sequences in East Africa, or perhaps those in South Africa with its emerging independent radiometric chronology. The relatively recent development of cosmogenic dating of fluvial terrace deposits (e.g., Wolkowinsky and Granger, 2004) offers a potential release from the dependency on long-distance cross-correlations for dating the many fluvial and open sites that comprise the African Stone Age record. As a case study, the Luangwa Valley project should be considered a preliminary test of the methodology under less than ideal conditions, as described below. The project was designed to provide independent checks on the cosmogenic results by applying isothermal thermoluminescence (ITL) dating and comparison against the magnetostratigraphy of the sedimentary

sequence. A description of the site formation precedes the artefact analyses and dating results. The paper concludes with a discussion of the archaeological significance of the lower Mode 1 gravels given the remaining uncertainties of the numerical age of the deposit.

The Luangwa Valley and the Manzi River section

The Luangwa Valley forms a 700 km long spur off the Western Branch of the East African Rift system (Dixey, 1937; Vail, 1969) that cuts diagonally (southwest to northeast) through the high central plateau of Zambia. The Valley currently supports dense concentrations of large herbivores that thrive on the comparatively nutrient rich soils and permanently available sources of surface water in the form of the Luangwa River, its perennial tributaries, and springs distributed along the Valley's flanks (Astle, 1971; Trapnell, 1996). By contrast, the Zambian central plateau has nutrient poor soils and consequently a low herbivore biomass despite its higher rainfall (East, 1984:246). Assuming a similar abundance of food resources in the past, the Luangwa Valley would have offered a natural corridor for hominin dispersals into southern or eastern Africa in an otherwise resource limited region. This hypothesis formed part of the basis of investigations begun in 2002 (below) to establish a chronological and palaeoenvironmental framework with which to assess the long-term human use of the Valley.

Although the Luangwa Valley is part of the Rift Valley system, it lacks the morphological structures that support the formation of closed lake basins and the volcanism that has enabled the development of long chronostratigraphic records from the Miocene through the Pleistocene in eastern Africa (Trauth et al., 2007). The Luangwa half-graben is marked by the steep Muchinga escarpment along its northwest margin that rises 800 m above the valley floor. The southeast margin is typically less clearly defined by broken ranges of hills. In the study area, the Nchindeni Hills are the exception as they form a 400 m high margin of Pre-Cambrian granites that parallel the Muchinga escarpment and constrain the course of the Luangwa River for approximately 35 km (Drysdall and Weller, 1966). The Luangwa Valley also differs from the deep sedimentary basins of the Eastern Rift in having generally thin mantles of Quaternary deposits; these are rarely more than 10 m deep and typically lie unconformably over Karoo Group (Permian-Triassic) sediments that form the Valley floor (Utting, 1988). Alluvium up to 37 m in thickness has been reported from exploratory petroleum cores (ITT, 1992), but these deep deposits are not exposed or accessible without substantial excavation. Aggressive erosion by the modern Luangwa River (Gilvear et al., 2000) combined with relatively little uplift creates secondary archaeological and palaeontological deposits in the current floodplain, and these are most commonly exposed in seasonal tributaries that drain the escarpments. The recovery of a fossilised femur of the Plio-Pleistocene primate *Theropithecus darti* and of Mode 1 cores on sand bars flanking the main river channel (Elton et al., 2003) highlights the potential of the Valley as a source of palaeoanthropological sites as well as the challenges of locating and dating intact deposits.

Before 2002, no excavation had been undertaken in the Luangwa Valley, with reports of Sangoan and potentially earlier sites based solely on surface finds (Macrae and Lancaster, 1937; Clark, 1954). A five-year programme of systematic survey and excavation began in 2003 in the South Luangwa National Park and in the adjacent Nchindeni Hills. Mode 1 cores and flakes were found eroding from gravel deposits exposed by the Manzi River ($S13^{\circ}11'58.6''$, $E31^{\circ}41'2.3''$), an ephemeral tributary of the Luangwa River (Fig. 1). The Manzi rises ~ 18 km to the northwest and is fed by wet season runoff from low-lying ridges that parallel the strike

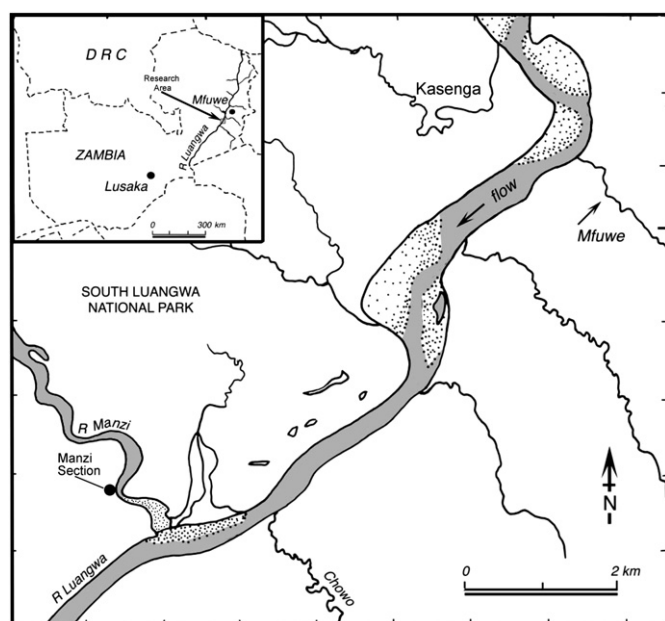


Fig. 1. Location of the Manzi River section in relation to the main channel of the Luangwa River, Zambia.

of the Valley. Near its confluence with the Luangwa, the Manzi has eroded a vertical bank into the undulating landscape, creating a section face that extends 160 m and varies 7.5–9 m in height (Fig. 2). The basal 3 m consist of Karoo Group mudstones which are of no archaeological interest, and these are overlain by ~4.7 m of artefact-bearing fluvial sands and gravels capped by a lag deposit also with artefacts. The 4 to 5 m difference in height between the Karoo bedrock and the Luangwa main channel may be protecting the overlying fluvial sediments from the most destructive effects of flood season discharge, but the Manzi in flood scours the Karoo base creating an unstable section face. The Karoo exposure is also undermined by elephants seeking mineral salts, and their digging contributes to localised section collapses. Parts of the section face have as a result retreated by up to 2 m between 2003 and 2008, and the artefact-bearing gravel beds described here no longer survive. This erosional process may typify the exposure and rapid loss of archaeological deposits along the Luangwa River and its tributaries. If so, the search for archaeological and palaeontological sites will involve a large element of luck in locating surviving deposits.

The Manzi River fluvial sequence is characterised by gravel lenses 15–20 cm thick that rest on local unconformities with lithologies dominated by well-rounded quartzite clasts with intermediate axes of 2–10 cm. Coarse to medium-grained sand lies gradationally over the gravels and fines upward. In profile, these sedimentary packages have lenticular shapes and are discontinuous laterally. The maximum thickness varies considerably along the section and is controlled by the amount of sand present between gravel layers. Cross bedding is present in both sand and gravel units. Based on observations of present-day sedimentary environments of the Manzi and Luangwa rivers, the gravels are inferred to be bars deposited by scouring wet-season floods.

An unconformity at ~200–210 cm divides the fluvial gravels into two sequences. It is identified by a 10 cm thick sub-horizontal silty clay layer (unit CL4) with dense concentrations of angular clasts, including artefacts, against which lower bedding forms truncate. This feature is observable across at least 75 m of the exposure (Fig. 2) and probably represents a relatively long-exposed former ground surface. The interlocking clasts suggest the formation of a pavement or lag deposit similar to that which caps the Manzi sequence today. Above the unconformity, a colourful soil overprints the uppermost 1–2 m of the section. The soil is characterised by a deeply reddened (2.5YR5/6 to 5YR4/4) Bt horizon in which pedogenic Fe-oxides and clay coat quartz grains. This is overlain by several cambic (Bw) horizons (7.5YR4/2) and a thin dark grey AB horizon (10YR4.2). The latter is rich in charcoal fragments. Beneath the soil horizon, the unweathered to lightly weathered (C or BC horizon) fluvial deposit is light grey (10YR6/3).

Quartzite cobbles with flake scars (cores) and flakes are evident in the lower gravel lenses and occur sporadically or, more rarely, as discrete clusters within the lenses. Given the fluvial origin of the gravels, the possibility exists that some of the apparent artefacts are simply the by-products of a highly active flow regime with non-artefactual flakes and cores formed by water-born impact. Before excavations began, a simple methodology was devised to minimise the inclusion of naturally flaked cobbles in the analysis. Fluvial processes can result in edge flaking of cobbles (Shackley, 1978; Schnurrenberger and Bryan, 1985; Gillespie et al., 2004), and the active seasonal flood regime of the modern Luangwa and its tributaries (Gilvear et al., 2000) have the potential to create assemblages of geofacts. A gravel bar at the junction of the Luangwa with the Fiya River, a tributary prone to flash floods, was sampled to characterise the frequency and extent of modification of clasts exposed to high velocity floods. Two 1 m² units were demarcated, and all surface clasts were collected and examined for signs of

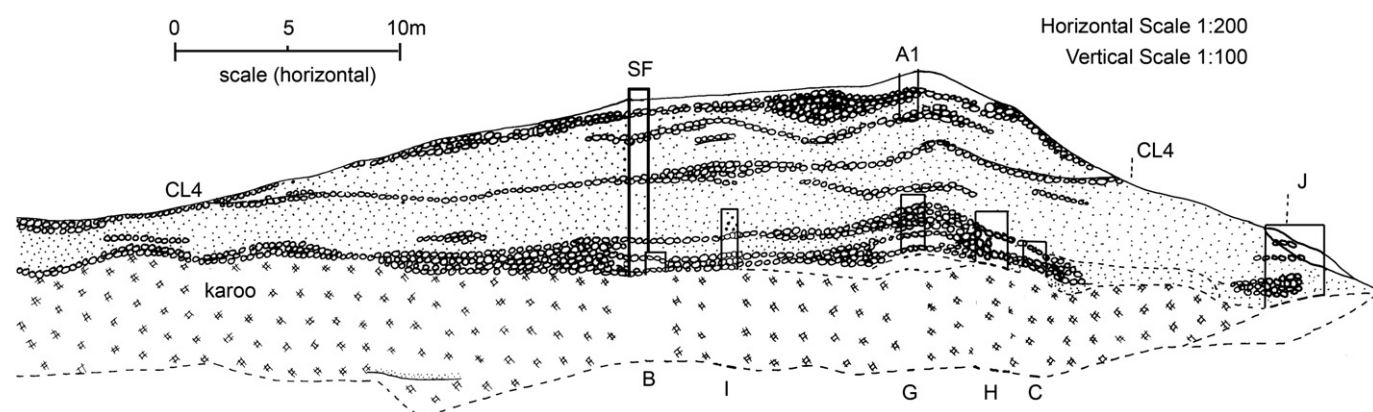


Fig. 2. Section drawing of the northern half of the Manzi River face, spanning approximately 75 m, showing gravel lenses (cobble layers) and the location of eight excavation units, including the full sequence sampled at SF and the upper deposits sampled in A1. Cobble Layer 4 (CL4) is highlighted as a marker horizon that separates the upper and lower units. These fluvial deposits lie unconformably over Karoo Group mudstones.

modification such as breakage or flake removals. Of the total of 468 clasts, 9.6% were modified ($n = 45$; 39 quartzite, 6 quartz). A further analysis of the damage patterns shows that 4.3% ($n = 20$) were cobbles split on the long axis; 2.1% ($n = 10$) were cobbles with one flake scar; 0.4% ($n = 2$) were cobbles with two flake scars; 1.5% ($n = 7$) were angular fragments; 1.0% ($n = 5$) were flakes lacking bulbs of percussion; and only 0.2% ($n = 1$) had a clear bulb of percussion. Among the clasts with flake removals, the majority ($n = 7$) had shallow or skimming flake scars indicative of glancing blows, and the remainder ($n = 12$) had scars ending in angular step fractures indicative of the force driven into the body of the clast (Cotterell and Kamminga, 1979). Absent were the deep scars with clear negative bulbs of percussion that occur typically as a result of intentional hard hammer knapping (Newcomer, 1971).

The predominance of shear fractures among the split cobbles could be interpreted as evidence of bipolar flaking (Barham, 1987), but the absence of further modification suggests these are naturally occurring breaks. This collection of fluviially damaged clasts provided practical guidelines for analysing the material excavated from the Manzi River section. All clasts with a single flake removal were discarded, even at the risk of losing genuine artefacts, and the frequency of split cobbles was treated as a potential indicator of flow strength involved in the formation of the lenses. The degree of rolling of likely artefacts was also recorded as an indicator of depositional history, with a sliding scale from fresh to heavily worn (see below). All sediments were sieved through a 3 mm mesh where possible to recover the small debitage indicative of knapping and as a measure of the winnowing of the deposits by flowing water (Sheppard and Kleindienst, 1996; Pavlish et al., 2002).

Excavation units and formation processes

The primary area selected for excavation in 2003 contained a representative sequence of gravel lenses within 4.7 m of sediment. Six upward fining packages of gravels and sands were recognised and numbered in descending order as cobble layers (CL) 1–6 (Fig. 3). CL1 differed from the other layers in having a more diffuse scatter of artefacts in contrast to the artefact clusters found in the lower layers. Scaffolding was erected to give access to the section face from the top to the basal contact with the Karoo. A vertical trench labelled SF (1 m × 0.5 m × 5 m) sampled the full sequence with each cobble layer treated as a natural excavation unit within which arbitrary spits were excavated if the unit exceeded 10 cm in thickness. The sterile sands separating the cobble layers were excavated in arbitrary units. The upper 1–2 m of fluvial sediments imprinted by the red soil development could be trowelled, but the underlying grey sands were indurated and had to be removed by hammer and chisel or by careful picking. No artefacts were found in the 1.8 m of sands that separated CL4 and CL5, and systematic sieving was applied only to alternating bucket loads. Across the Manzi section, a further seven 1 m wide vertical trenches were established to maximise the sample of artefacts from the two lowest cobble layers (CL5 and CL6), and one was extended to include the unconformity recognised as CL4. In 2004, a 1 m × 2 m long trench (A1, Fig. 2) was opened on the surface of the highest point of the section to provide sediment samples for luminescence dating and in situ dosimetry data (see below). A1 was excavated to a depth of 135 cm below ground level, sampling the red soil and the top of the underlying unweathered sands and incorporating stratigraphic units equivalent in depth to CL1–CL3 in the main trench, SF.

Artefact frequencies were low in each of the cobble layers of the main section (Table 1). These results support the initial impression of scattered artefact occurrences within lenses with some having denser concentrations, as seen in CL1 and CL2. The small sample

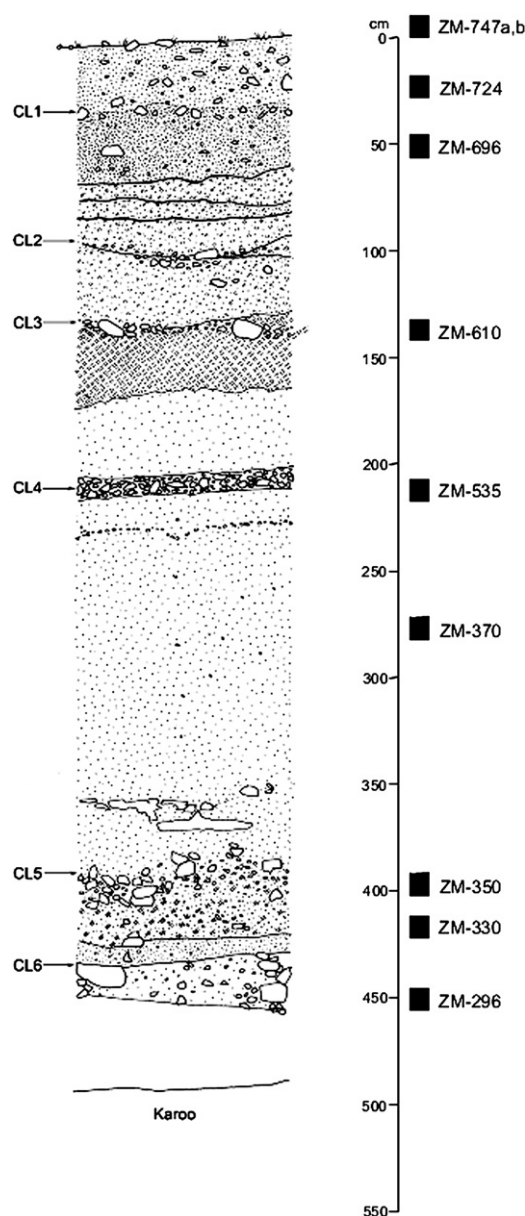


Fig. 3. Main section (SF) stratigraphic sequence showing the position of cobble layers (CL1 to CL6) above Karoo Group deposits and the location of sediment samples collected for cosmogenic nuclide dating.

sizes and absence of retouched tools in CL1–CL4 makes it difficult to attribute these assemblages to particular industrial traditions in the south-central African archaeological record. As a generalisation, retouched tool frequencies are low in mid- to late Pleistocene assemblages in the region, with the consequence that comparative techno-typological analyses generally rely on indirect indicators of shifting reduction strategies (Barham, 2000). In particular, the technological attributes of cores are used as proxies for attributing assemblages to general Modes of production (after Clark, 1969), and this approach is followed here. For purposes of comparative statistical analysis of the upper and lower Manzi sequence, CL1–CL4 are treated as a single analytical unit representing assemblages above and including the unconformity. CL5 and CL6 are retained as separate layers representing the sequence below the unconformity. Artefacts from the other seven excavation trenches are assigned to CL4, CL5, and CL6 based on stratigraphic

Table 1
Manzi River main section artefact frequencies (SF) for cobble layers (CL) 1–6^a

Cobble layer reduction category	CL1	CL2	CL3	CL4 ^b	CL5 ^b	CL6 ^b
Whole flakes	22	5	4	3/1	3/20	5/25
Broken flakes	7	8	1	0	1/1	0
Shatter <20 mm	18	12	3	0	0	1/4
Angular chunks	5	1	0	0	0/2	1/3
Cores	5	3	1	3/2	0/8	1/5
Edge damaged/used	0	0	0	0	2/4	2/5
Retouched	0	0	0	0	0/2	1/2
Total	57	29	9	6/3	8/37	12/44
Split cobbles	3	0	0	0/1	0/3	1/4

^a Split cobble frequencies are not included in the total but are presented as a possible indicator of fluvial activity.

^b Indicates layers which incorporate artefacts from all excavation units across the site, and these additional totals are listed after each main section total (main section face/all other excavation units).

correlations across the section with the result that artefact totals become comparable for the aggregated upper ($n = 104$) and lower units ($n = 101$; Table 1).

Before making comparisons between units, some assessment is needed of the impact of the formation of the gravel lenses on the integrity of the archaeological content. As discussed above, the modern gravels of the Luangwa contain a small percentage of modified clasts (<10%), of which split cobbles predominate. In the upper unit of the Manzi section, split cobbles occur in CL1 and CL4 (Table 1) which suggests CL2 and CL3 may have formed under lower energy conditions, but the area sampled is very small and this interpretation is necessarily provisional. Split cobbles occur in the combined CL5 and CL6 data set but are rare in the main section excavation (Table 1). A more reliable indicator of the extent of re-deposition in these assemblages is the frequency of surface damage resulting from movement and sediment compaction (Andrews, 2006). All modified clasts examined in the Luangwa river control

sample showed signs of edge damage resulting from abrasion, which is not surprising given the coarse sand and gravel matrix of the deposit. An index of edge (arrête) and flake scar ridge (arris) alteration was applied to the Manzi archaeological assemblages based on a qualitative set of criteria developed for describing artefacts from secondary depositional contexts at Kalambo Falls, Zambia (Clark, 1974:103). Five categories were devised representing a gradation of edge abrasion from fresh (no visible abrasion), sharp (slight abrasion), moderately worn (uneven abrasion with mix of wear to edges), worn (more uniform rounding of surfaces), and heavily worn (ridges rounded to nearly flattened). These categories were applied to cores and whole flakes (Figs. 4 and 5). The upper unit has a higher proportion of fresh to sharp artefacts with more moderate to heavy wear in the lower unit. Some of this difference may reflect the extent of abrasion from sediment compaction, with the older lower deposits experiencing more modification with time. Within the lower unit, CL6 artefacts tend to be less worn than those in CL5 which suggests a genuine difference in formation histories. The CL6 gravels may have been buried relatively rapidly and protected from aerial weathering or fluvial transport and winnowing. The presence in CL6 of five pieces of small knapping debitage (<20 mm; Table 1) provides additional, though limited, support for the interpretation of a more protected depositional context. Similarly, the comparative abundance of small knapping debris in CL1 and CL2 correlates with a higher frequency of fresh to sharp artefacts in these upper cobble layers. No refits of flakes to cores were found, which is not surprising given the small exposures investigated and the fluvial contexts of the finds.

All artefacts are assumed to be in secondary contexts and subjected to varying degrees of transport from the point of manufacture, use, or discard. Those in the upper unit, in particular from CL1, have suffered the least damage and presumably the least movement while those from CL5 show the greatest abrasion. The

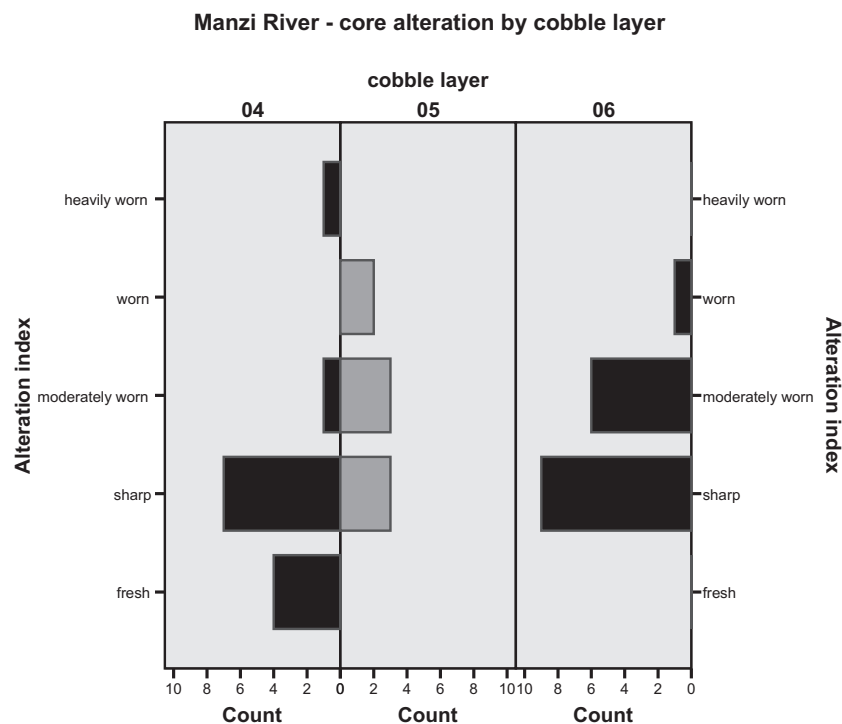


Fig. 4. Core edge alteration index frequencies for the upper and lower units (upper unit = 04, lower units represented by 05 [CL5] and 06 [CL6]). Core surfaces are most heavily abraded in CL5 and least abraded in the upper unit.

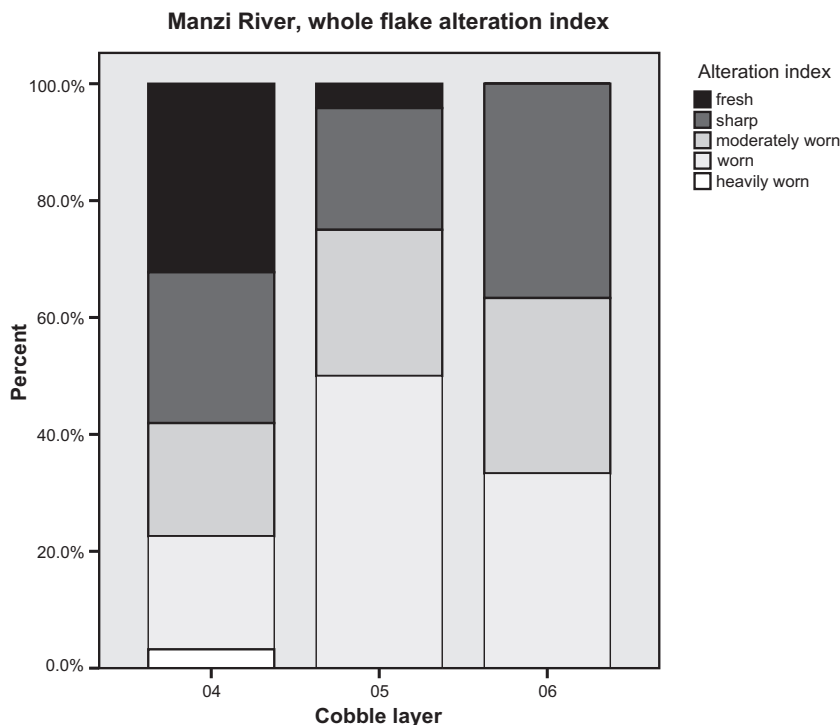


Fig. 5. Flake alteration (abrasion) frequencies in the upper unit (04) and the lower unit (05, 06). Flakes are generally less abraded in the upper unit, and in the lower unit CL5 flakes are generally more abraded than those in CL6.

generally higher levels of abrasion in the lower layers may also reflect the greater age of these deposits as they will have been exposed to more episodes of fluvial reworking and surface wear through compaction of the enveloping coarse sediments.

The occurrence of artefacts in each cobble layer with varying levels of abrasion also highlights the likely complex history of gravel formation combined with periodic hominin use of the gravels as a raw material source. The modern Manzi and Luangwa gravels, as analogues of Pleistocene deposits, provide examples of seasonally available and easily accessed gravels with abundant siliceous materials (quartzite and quartz) for tool making. Other local sources of similar raw materials include the perched gravel ridges which form the headwaters of the Manzi today. Primary sources of quartzite and vein quartz occur in the flanking escarpments of the Luangwa Valley, with the Nchindeni Hills at a distance of 10 km being the nearest source. Access to the Nchindeni today from the Manzi involves crossing the main channel of the Luangwa River, which presumably would also have been the case in the late Pleistocene, if not earlier. Nearby and on the Manzi side of the Luangwa are dolerite dikes and chert sills, both exposed 5 km northeast of the Manzi section at Chichele Hill, a Pre-Cambrian feature (Utting, 1988). These rocks are rare in the excavated units (below) but appear to be absent in the modern Manzi gravels based on surface surveys.

In summary, the artefact units with their varied abrasion indices represent multiple episodes of largely fluvial transport, but among the less abraded and presumably less transported pieces exists potential evidence for hominin selection and use of raw materials. More valuable at this early stage of exploration in the Luangwa Valley is the general culture-stratigraphic sequence preserved in the Manzi section. That sequence is clearly coarse-grained and discontinuous, but it forms the basis of an initial framework for ordering the earlier archaeological record of the Valley. That sequence is outlined below followed by the results of the dating programme.

Artefact analysis

Given the rarity of retouched tools and the small sample sizes in each cobble layer, the analysis here uses changing patterns of flake production as the basis for comparing the upper and lower cobble layers. In particular, emphasis is given to the presence of core preparation as a marker of Mode 3 (Middle Stone Age) technologies, although we are aware that core preparation is not an exclusively Mode 3 phenomenon as it occurs in later Mode 2 assemblages elsewhere in Africa (Sharon and Beaumont, 2006). No Mode 2 bifaces (handaxes, cleavers) were recovered in the Manzi sequence, and none were found in the streambed or in the immediate landscape behind the section. Mode 1 flaking is a basic reduction technique that occurs from the outset of the African archaeological record (Delanges and Roche, 2005) and remains part of the technological repertoire into much later periods (Gowlett, 1986). In the context of this study, the only criterion that might distinguish between the predominance of Mode 1 or Mode 2 is flake size, with Mode 2 assemblages often associated with larger flakes (>10 cm) than Mode 1 assemblages (Clark, 2001b). Unfortunately, in the Luangwa Valley no excavated Mode 2 assemblage is available as a reference collection for discriminating between Modes based on flakes and cores alone. Raw material size limitations may have restricted the production of biface flake blanks, but suitable clasts do exist in the modern Manzi gravels and did so prehistorically, as evidenced by a large quartzite core in CL6 (13.7 cm × 10.8 cm × 7.8 cm; Fig. 6B).

Although the sample size of cores is too small to support meaningful statistical comparisons, there are nonetheless discernible differences in the sequence (Fig. 7). Prepared cores occur only in the upper unit, particularly in CL1–CL3 (Fig. 6N). Finer-grained raw materials (chert, quartz crystal) are also most common in the upper unit (Table 2; Fig. 6L and M). The only core of coarse-grained dolerite comes from the basal layer (CL6), and also distinctive to the lower unit are split cobbles with centripetally

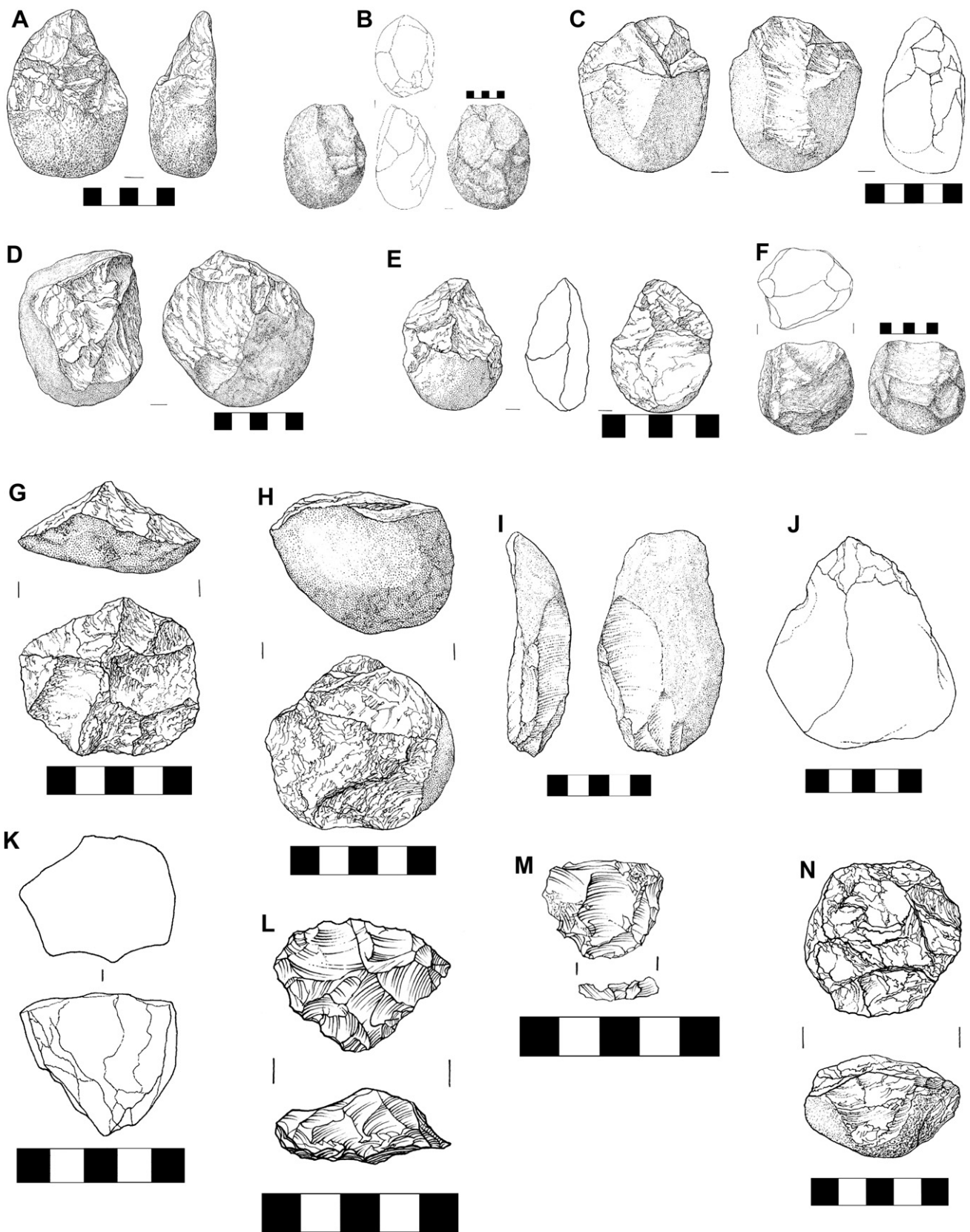


Fig. 6. Artefacts from the Manzi River main section (SF) and other excavation units listed by cobble layer: A, quartzite core/pick from CL5 (SF); B, large quartzite core/chopper, CL6 (SF); C, quartzite core/chopper, CL6; D, quartzite core, CL6; E, quartzite multiple platform core, CL6 (unit i); F, quartzite opposed platform core/chopper, CL4 (unit h); G, quartzite centripetally flaked core (disc) on split cobble, CL6 (unit h); H, split quartzite cobble core with centripetal flaking, CL6 (unit e); I, retouched quartzite flake (sidescraper), CL6 (unit j); J, quartzite pick shown in outline, CL6 (unit b); K, vein quartz blade/flake core shown in outline, CL2 (unit A1); L, endshock fragment of chert radial core that has been re-flaked, CL1 (SF); M, chert flake with multi-facetted butt, CL2 (SF); N, vein quartz prepared core, CL3 (SF).

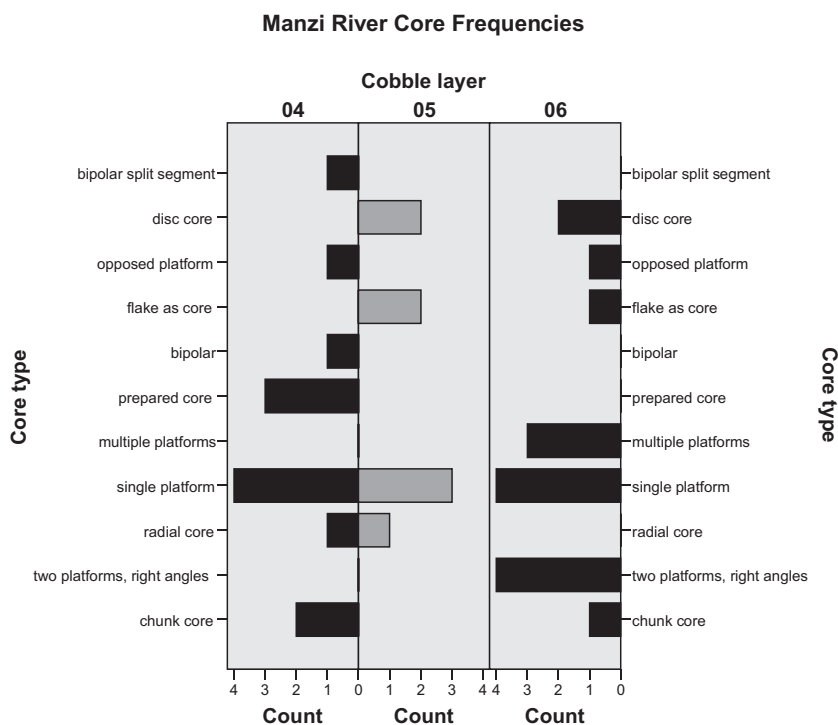


Fig. 7. Core type frequencies in the combined upper unit (04) and in the two lower unit cobble layers 5 (05) and 6 (06).

flaked surfaces (disc cores; Fig. 6G) and multiple platform cores (Fig. 6E).

The more numerous sample of whole flakes provides further support for a technological separation between the upper and lower units. The majority of flakes in all layers are made on cobbles and show the characteristic cortex on the dorsal surface and cortical butts of initial stages of flaking (Figs. 8 and 9; Toth, 1985), but clear differences exist in dorsal scarring and in approaches to butt preparation. Dorsal scar patterns show greater variability in the upper unit, including the only occurrences of a convergent Levallois pattern (Fig. 8). Multi-faceted and simple faceted butts occur primarily in the upper unit (Figs. 6M and 9) including

a faceted chert blade. A techno-morphological classification of flakes (Fig. 10) shows a greater variety of types occurring in the upper unit, including a faceted flake, a blade, and the presence of pentagonal shapes typically linked to centripetal flaking and Mode 3 technologies in central Zambia (Barham, 2000:108). Mean flake dimensions (Table 3) also differ between the upper and lower units with flakes in the lower unit being significantly longer, wider, and thicker (Levene tested for equality of variance with the null hypothesis supported in each comparison; between group ANOVA length [d.f. = 1, $F = 7.573$, sig. 0.003]; width [d.f. = 1, $F = 7.778$, sig. 0.007]; and thickness [d.f. = 1, $F = 9.248$, sig. 0.003]). Raw material frequencies also differ between units with vein quartz accounting

Table 2
Crosstabulation of core type and raw material for the combined upper unit (04) and lower unit cobble layers 5 (05) and 6 (06).

Cobble layer		Raw material					Total
		Quartz crystal	Vein quartz	Quartzite	Chert	Dolerite	
04	Type	Chunk core	0	1	1	0	2
		Radial core	0	0	0	1	1
		Single platform	1	1	2	0	4
		Prepared core	0	1	2	0	3
		Bipolar	1	0	0	0	1
		Opposed platform	0	0	1	0	1
		Bipolar split segment	0	0	1	0	1
		Total	2	3	7	1	13
05	Type	Radial core	1	0	0	0	1
		Single platform	0	0	3	0	3
		Flake as core	0	0	2	0	2
		Discoidal core	0	0	2	0	2
		Total	1	0	7	0	8
06	Type	Chunk core	0	1	0	0	1
		Two platforms, right angles	0	0	3	1	4
		Single platform	1	1	2	0	4
		Multiple platforms	0	0	3	0	3
		Flake as core	0	0	1	0	1
		Opposed platform	0	0	1	0	1
		Discoidal core	1	1	1	0	2
	Total	1	2	12	1	16	

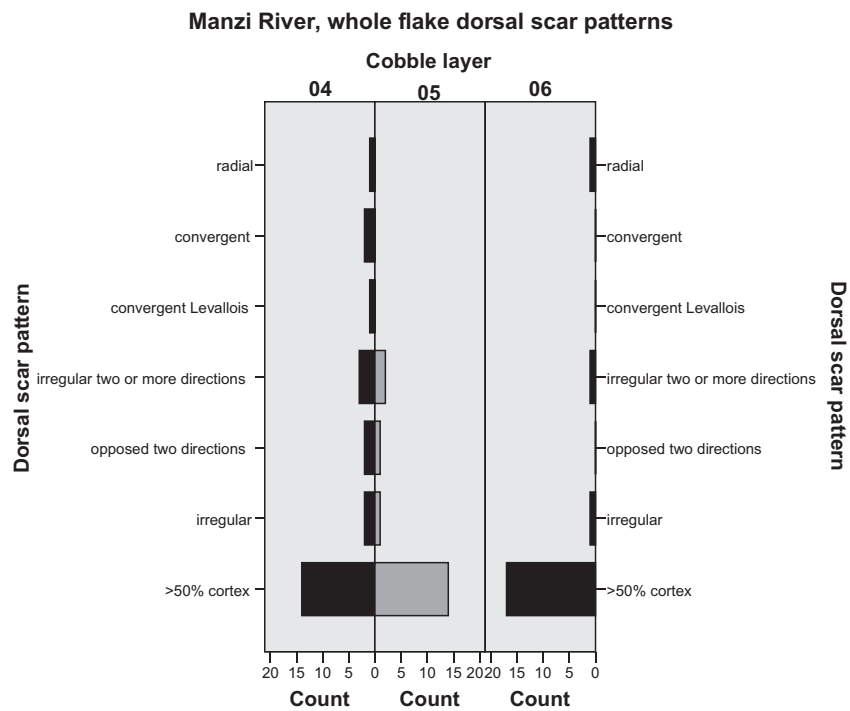


Fig. 8. Frequencies of dorsal scar patterns on flakes in the combined upper unit (04) and in the lower unit cobble layers 5 (05) and 6 (06).

for 50% of flakes in the upper unit ($n = 15$) and 38% ($n = 11$) in CL6. Quartzite is also more common in the lower unit flakes in keeping with the prevalence of coarser-grained materials among basal layer cores.

Among the small sample of modified/used pieces, a faceted convergent flake occurs in the upper unit, and the lower unit contains the only spheroid found. Hammerstones, including

a pitted hammerstone/anvil (Fig. 11), were found in the lower unit. In such small numbers these artefacts are not particularly informative, but when considered in relation to the distinctions observed among the cores and flakes they add to the overall technological patterning which separates the upper from the lower unit. The presence of retouched tools in only the lower unit precludes any discussion of temporal patterning, and there are no

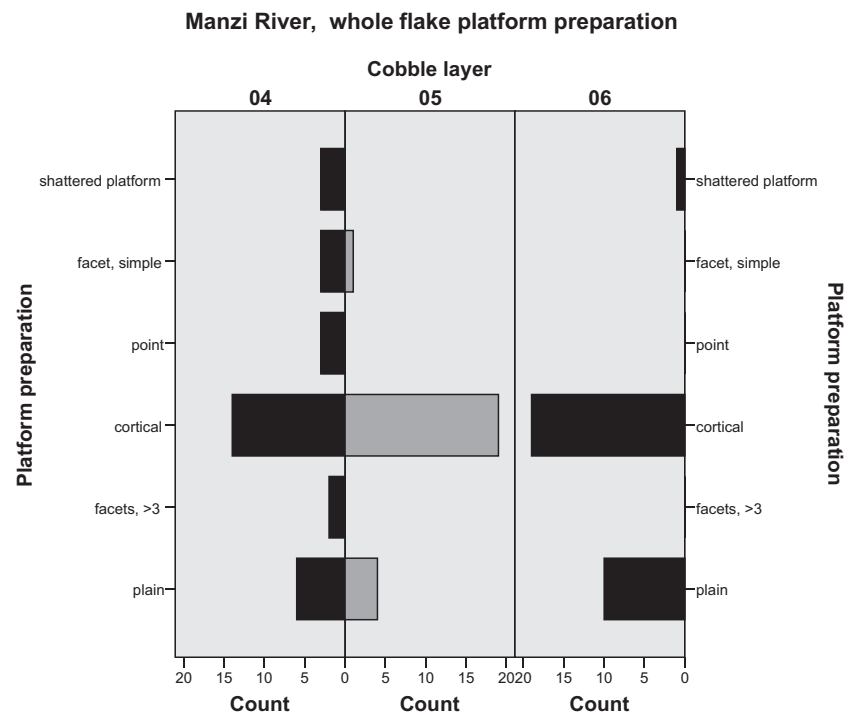


Fig. 9. Frequencies of types of platform preparation on flakes from the combined upper unit (04) and from the lower unit cobble layers 5 (05) and 6 (06).

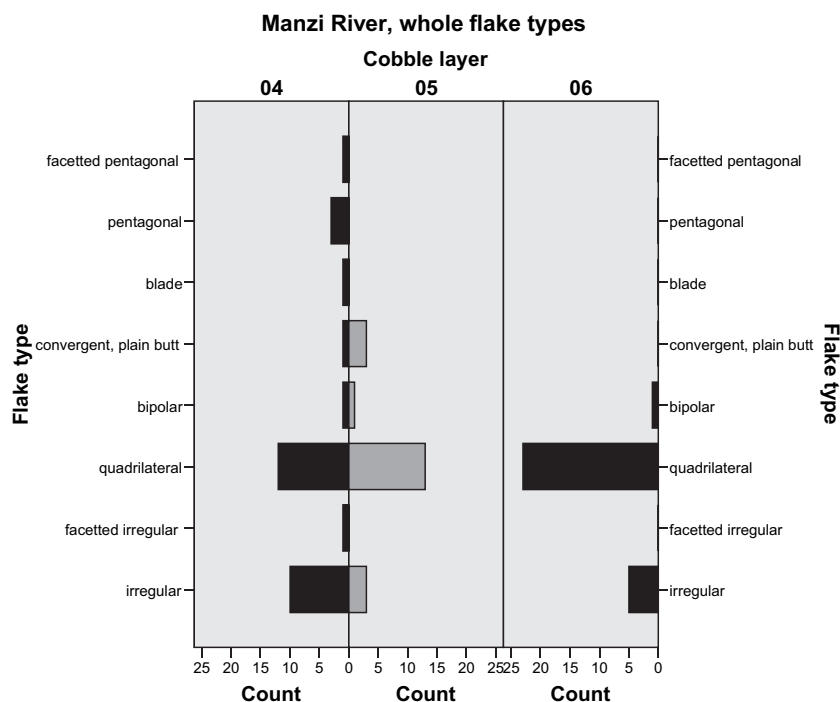


Fig. 10. Frequencies of flakes by morphological type in the combined upper unit (04) and in lower unit cobble layer 5 (05) and 6 (06).

distinctive Mode related types (two scrapers, two pick-like cores, and one naturally backed knife (Fig. 6A, I and J)).

The interpretation offered of the above data is one of a basic separation of Mode 3 technology above the unconformity (CL4) and Mode 1 technology below. The sample of artefacts from the unconformity itself is too small to attribute to either Mode, but a large opposed platform core/chopper (quartzite) was found at the base of the layer (Fig. 6F) and is more abraded than the flakes occurring on the layer's surface. A considerable chronological gap appears to be represented by this lag deposit, which is interpreted to be an old ground surface. Before turning to the dating results, the age of the Manzi sequence can be very roughly estimated by correlation with the few numerically dated sites in south-central Africa and further afield in eastern and southern Africa. Such estimates highlight the inherent limitations of sequence building in the absence of directly applicable dates. For the upper unit, the only numerically dated Mode 3 assemblages in the immediate region are from the Zambian sites of Twin Rivers Cave and Mumbwa Caves (Barham, 2000). Based on these two sites, the age of the upper unit could be as old as ~265 ka but is probably not younger than ~30–25 ka. Later mid-Pleistocene Mode 3 assemblages are well documented from the Kapthurin Formation, Kenya (Tryon and McBrearty, 2006), and have been reported from Wonderwerk Cave, South Africa (Beaumont and Vogel, 2006), and provide support for an early and widespread occurrence of Mode 3 technology from eastern to southern Africa (Barham and Mitchell, 2008:233). The lower unit at Manzi is stratigraphically earlier, but the potential chronological boundaries are wide given the longevity of Mode 1 technology as a basic reduction strategy. The age range could transcend the Oldowan (2.6–1.7 Ma) and extend through the Acheulean (~1.7–0.3 Ma). If the lower unit represents a context specific variant of Mode 2 in which hominins rarely made bifaces, as in the case of the mid-Pleistocene of the Olgosailie Basin, Kenya (Potts et al., 1999) or in the British Clactonian (Wenban-Smith et al., 2006), then the age of the lower unit could post-date the Oldowan. These chronological uncertainties emphasise the interpretive challenges facing

archaeologists in the absence of well-developed local chronological frameworks, and in the case of south-central Africa there are no securely dated Mode 1 assemblages.

The following sections present the methodologies, results, and age interpretations for the cosmogenic nuclide dating of the lower and upper units along with the magnetostratigraphy of the full sequence. The polarity record of the sediments provides a relative age sequence for comparison with the cosmogenic estimates. Isothermal thermoluminescence (ITL) analysis was undertaken on upper unit sediments, and the results offer an independent check on the attempt to calculate cosmogenic exposure ages of these gravels.

Cosmogenic nuclide dating of the Manzi section—methods

Alluvium can be dated in some situations using exposure dating in which the accumulation of cosmogenic nuclides in surface-exposed materials is measured. Exposure dating methods involving sampling of surface clasts (e.g., Bierman et al., 1995) or shallow

Table 3
Mean and standard deviation of flake dimensions (length, width, and thickness) for whole flakes from the upper unit (04) and the lower unit cobble layers 5 (05) and 6 (06)

Cobble layer		Length	Width	Thickness
04	Mean	34.68	31.77	10.45
	n	31	31	31
	Std. deviation	16.071	12.511	5.881
05	Mean	49.21	47.13	15.63
	n	24	24	24
	Std. deviation	16.202	14.522	5.962
06	Mean	41.90	37.80	14.87
	n	30	30	30
	Std. deviation	17.343	17.024	8.345
Total	Mean	41.33	38.24	13.47
	n	85	85	85
	Std. deviation	17.383	15.867	7.177

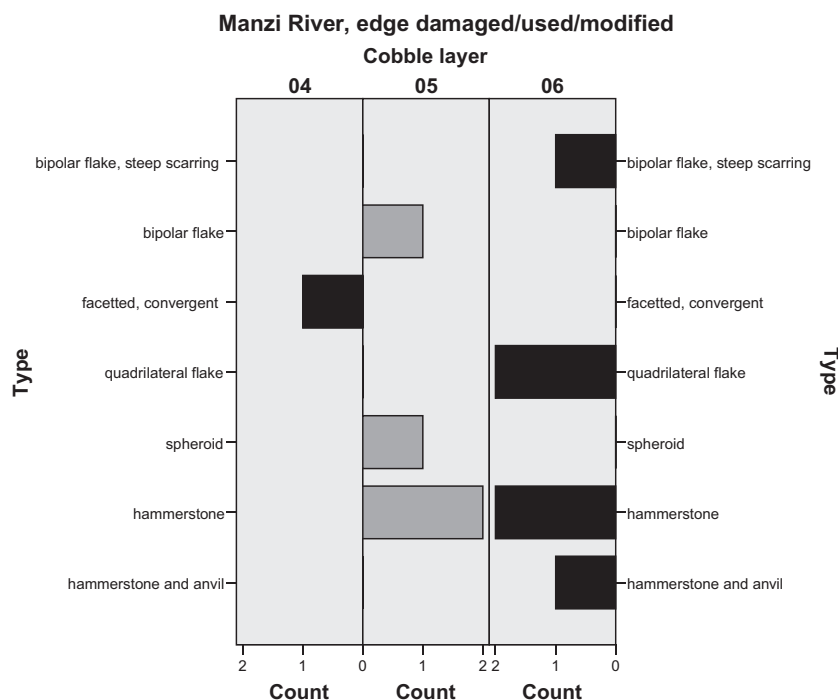


Fig. 11. Frequency of edge damaged or modified artefacts in the combined upper unit (04) and in lower unit cobble layer 5 (05) and 6 (06).

depth profiles (e.g., Anderson et al., 1996; Phillips et al., 1998) have been widely employed. Exposure dating has proven useful for alluvium that has experienced little disturbance from erosion, burial, or bioturbation following deposition. However, the requirement for preservation of near-original surfaces generally limits exposure dating to relatively young deposits of a few 100 ka or less.

More recently, burial dating of alluvial deposits using cosmogenic ^{26}Al and ^{10}Be in a deep vertical profile has been used for older deposits (Granger and Smith, 2000; Granger and Muzikar, 2001; Wolkowinsky and Granger, 2004; Balco and Rovey, 2008). Burial dating is relatively straightforward when the sample to be dated has experienced a simple two-stage geomorphic history. First, the nuclide inventory of the alluvial sample must have originated from a landscape of erosional equilibrium. This occurs when steady erosion proceeds for a long enough time that nuclide production is in equilibrium with loss from erosion and decay. Second, the sample must have been buried (and remained buried until the present time) at sufficient depth to significantly reduce further nuclide production. Sediment washed into a cave is one example of such a setting (Partridge et al., 2003; Chazan et al., 2008). In addition, the profile must consist of sediments emplaced over a relatively short time period (few tens of ka or less) with no significant unconformities (Hanks and Finkel, 2005). If such conditions apply, then a single sample can provide an estimate of burial time and erosion rate by exploiting the differential decay of ^{26}Al (half-life 0.705 Ma) and ^{10}Be (half-life 1.36 Ma). This scenario has been called “simple” burial dating in order to distinguish it from more complex settings (Balco and Rovey, 2008). Multiple samples taken over a depth profile can be used to correct for complications such as post-burial erosion of the top of the deposit (Wolkowinsky and Granger, 2004). A depth profile >10 m deep with at least five widely spaced samples should result in a robust estimate of buried sediment age, source region erosion rate, and alluvial terrace erosion rate (Granger and Muzikar, 2001).

Our sampling protocols were based upon this methodology and the geomorphic assumptions implied by it. At the time of sampling

in 2003, we were aware of several significant deviations from the ideal burial dating setting. The 4.7 m Manzi sequence is about half the depth of an ideal profile. In addition, we recognised an unconformity, representing an unknown amount of time, between the upper and lower portions of the section at ~200–210 cm depth. Consequently, we sampled a depth profile, surface sediments, and modern stream alluvium in an attempt to place broad limits on the age of the sequence. The burial dating technique was applied to SF, the section face excavation which exposed the full Manzi sequence. There is ample evidence that undercutting and slumping have recently exposed the Manzi section as a whole, making the exposure the natural equivalent of a road cut or mining core. The excavations added further insurance that the samples collected for analysis were freshly exposed.

Eight samples were taken from the profile (Fig. 3). Four samples lie below the unconformity between depths of 451–212 cm, and four were collected between depths of 212–23 cm. Each sample was taken from a restricted depth interval of ± 10 cm. Samples consisting of clasts were amalgamated by mass (Anderson et al., 1996) in the laboratory to provide an estimate of the average nuclide concentration at that depth. At several depth intervals, sand-sized material was obtained and amalgamation was not needed.

A sample of loose quartzite cobbles from the surface of the Manzi section was also analysed. These cobbles form an interlocking pavement on a gentle slope that is locally absent where vegetation is present. The absence of fines and the interlocking character of the cobbles suggest that this is a lag deposit formed by the steady erosion of the alluvial section. At least 3.8 m of sediment have been lost above the Manzi section based on our survey from the SF datum to the top of the adjacent hill. Fine grained sediment is readily transported off the surface by slope wash, raindrop splash, and wind, while the cobbles move more slowly and hence concentrate on the surface. This implies that the surface cobbles were derived from sediment formerly over the Manzi section. The surface sample consists of 35 randomly selected quartzite pebbles amalgamated by mass in the laboratory following crushing of the

clasts to sand size. This sample was divided into two aliquots for isotopic analysis (ZM-747a, b).

Finally, a sample of modern sand-sized alluvium from the active Manzi River channel was obtained. This sample was intended to establish a baseline for nuclide inheritance corrections for surface samples. It also provided a crucial test of our assumptions concerning the source and exposure history of the alluvium containing the Mode 1 artefacts.

Cosmogenic nuclide depth profile—laboratory procedures and analytical results

Following crushing and sieving, about 100 g of each sample (grain size 250–500 μm) was etched in solutions of HF and HNO₃ to yield highly purified quartz with total Al concentrations of <200 ppm. The sample was then dissolved in HF, spiked with 0.25–0.55 mg Be, and cosmogenic ¹⁰Be and ²⁶Al extracted following procedures modified from Bierman et al. (2002). No Al spike was required. Elemental Al concentrations were measured by Flame Atomic Absorption Spectrometry in which unknowns were bracketed by standards. Isotopes of Al and Be were measured by accelerator mass spectrometry (AMS) at the PSI/ETH facility in Zurich (Kubik et al., 1998). At the time of measurement, AMS standards used were S555 with a nominal value of ¹⁰Be/Be = 95.5 × 10⁻¹² and standard AL09 with a nominal value of ²⁶Al/Al = 1190 × 10⁻¹². Analytical results have been renormalised relative to standard 07KNSTD (¹⁰Be) and standard KNSTD (²⁶Al) to facilitate inter-laboratory comparisons and to use the latest decay constant information. Further analytical details are given in Table 4. The ²⁶Al analysis for sample ZM-724 yielded an unrealistically low ²⁶Al/¹⁰Be and is believed to be erroneous for unknown analytical reasons. It is not used in our interpretations. We were unable to obtain a ²⁶Al analysis for ZM-696 because of laboratory problems. The ¹⁰Be data for both SM-696 and SM-724 are fine.

Cosmogenic nuclide depth profile—results and discussion

Modern alluvium from the Manzi active channel (sample Manzi-1) has a ²⁶Al/¹⁰Be ratio of 4.93 ± 0.60 that plots well below the constant exposure-erosion island (Fig. 12). Such a plot indicates long burial. Ratios from samples below the unconformity have depressed ratios (samples ZM-296, ZM-330, ZM-350, and ZM-370; mean ratio = 4.95 ± 0.44) that also fall below the constant exposure-erosion island. Ratios from above the unconformity (samples ZM-610 and ZM-535; mean ratio = 6.18 ± 0.29) are distinctly different from lower samples. They plot on or very near

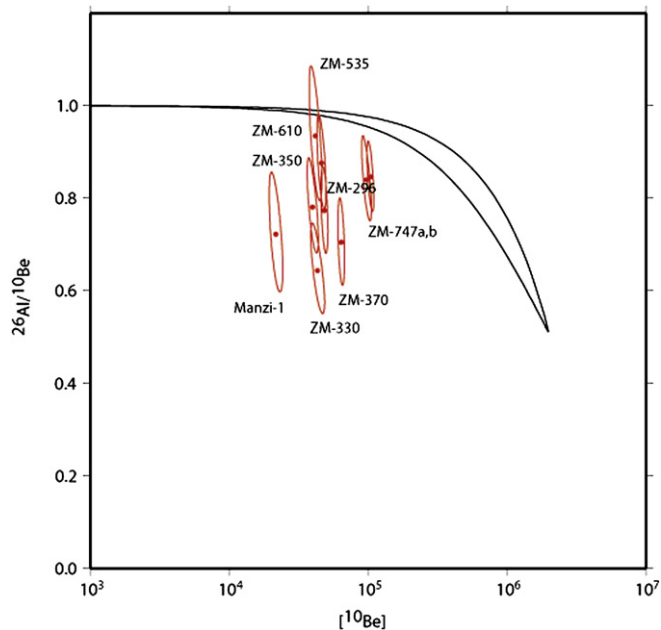


Fig. 12. Plot of ²⁶Al/¹⁰Be ratios versus ¹⁰Be concentration relative to standard 07KNSTD. The ellipses indicate 1σ analytical errors. Samples plotting below the constant exposure-erosion island (black lines) have experienced one or more periods of burial. Plot generated by the CRONUS-Earth ¹⁰Be–²⁶Al exposure age calculator (<http://hess.ess.washington.edu/>, v. 2.2).

the constant erosion-exposure island. These results suggest that the section consists of older deposits in which nuclide ratios have declined after long burial capped by younger deposits largely derived from a steadily eroding landscape. One interpretation is that gravels CL4, CL5, and CL6 are mainstream Luangwa deposits, while CL3, CL2, and CL1 are deposits of the Manzi River. Contrasts in raw material artefact frequencies between the two units support a difference in source regions. Alternatively, both units could be deposits of the Manzi River.

The analyses of surface clasts (ZM-747a, b) also show a depressed ratio (5.75 ± 0.02) below the constant erosion-exposure island. Geomorphic evidence for the origin of the surface clasts as a lag deposit suggests this is due to exhumation of previously deeply buried clasts.

Another important result is that the uppermost four samples (ZM-724, ZM-696, ZM-610, and ZM-535) have ¹⁰Be concentrations

Table 4
Cosmogenic ¹⁰Be and ²⁶Al concentrations in quartz from the Manzi River section^a

Sample	Depth (cm)	[¹⁰ Be] (10 ⁴ atoms g ⁻¹)	±	[²⁶ Al] (10 ⁴ atoms g ⁻¹)	±	²⁶ Al/ ¹⁰ Be	±
Manzi-1 ^b	–	9.35	0.72	46.07	4.38	4.93	0.60
ZM-747A ^c	0	44.73	1.74	258.28	12.14	5.77	0.35
ZM-747B ^c	0	41.95	2.31	240.56	12.03	5.73	0.43
ZM-724	23	19.02	0.84	46.68 ^d	3.78	2.45 ^d	0.23
ZM-696	51	22.41	1.12	nd	nd	nd	nd
ZM-610	137	19.89	1.01	118.92	7.25	5.98	0.48
ZM-535	197	18.00	1.35	114.90	9.19	6.38	0.70
ZM-370	377	27.58	1.05	132.70	11.01	4.81	0.44
ZM-350	397	17.20	1.12	91.70	5.87	5.33	0.49
ZM-330	417	18.67	1.44	82.02	5.50	4.39	0.45
ZM-296	451	20.87	0.81	110.19	7.93	5.28	0.43

^a Location of all Manzi section samples is 13.19961° south latitude, 31.68397° east longitude, surface elevation 529 m. Samples analysed at ETH-Zurich with standard S555 for ¹⁰Be (assumed ratio of 95.5 × 10⁻¹²) and standard ZAl94 for ²⁶Al (assumed ratio of 526 × 10⁻¹²). Concentrations have been normalised relative to standard 07KNSTD (¹⁰Be) and standard KNSTD (²⁶Al). See http://hess.ess.washington.edu/math/docs/al_be_v22/AlBe_changes_v22.pdf for details. Errors are 1σ and include analytical uncertainties only.

^b Sample from modern alluvium of the Manzi River.

^c Sample of surface clasts at top of Manzi section.

^d Analysis for ²⁶Al believed to be invalid.

that do not fall along an exponential trend despite being mostly contained in a well-developed soil. An exponential trend created by the near-surface dominance of neutron spallation is expected in shallow (<2 m) nuclide profiles. This could be explained by post-depositional vertical mixing of clasts by bio- or pedo-turbation (Balco and Rovey, 2008), significant differences in nuclide inheritance between samples, undetected unconformities (as suggested by archaeological and palaeomagnetic data), and/or recent erosional removal of the exponential trend.

Samples from deposits below the unconformity also do not exhibit an exponential nuclide concentration trend (Fig. 13). In addition, while showing evidence of post-depositional

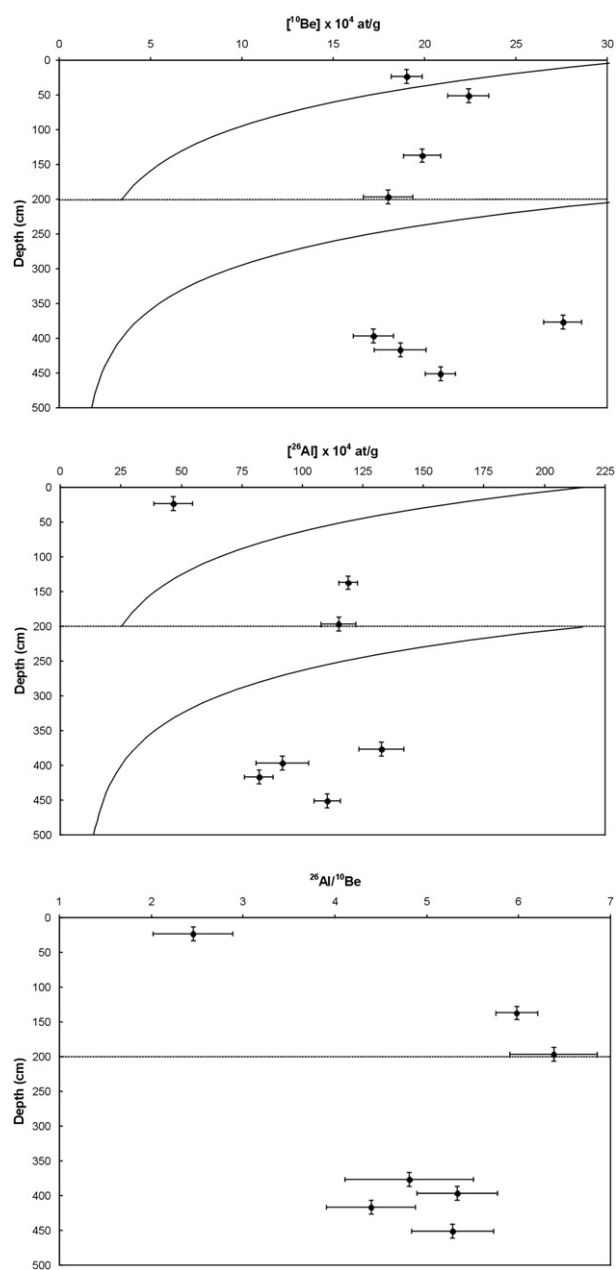


Fig. 13. Cosmogenic nuclide concentration depth profiles for the Manzi section. Error bars are 1σ analytical errors for nuclide concentrations and ± 10 cm for depth. Dashed lines show unconformity discussed in text. Curves show model profile concentrations for ^{10}Be and ^{26}Al for an arbitrary exposure period of 75,000 years. The upper line is computed from the present-day surface to depth of unconformity at 200 cm. The lower line depicts profile computed with the unconformity as the land surface.

cementation, there is no indication of a paleosol. This indicates that at least several metres of sediment were eroded from the lower unit before burial. This is significant because in some cases buried deposits preserving an exponential trend indicative of near-surface exposure and/or a paleosol can be burial dated (Balco and Rovey, 2008).

The validity of burial dating and surface exposure dating in this setting are challenged by these results. First, cosmogenic nuclide ratios support archaeological and geomorphological evidence for a considerable chronological gap across the unconformity separating the upper and lower units. The presence of this unconformity violates the requirement that the depth profile be taken across sediments of approximately the same age. A second challenge comes from the sample of modern alluvium with depressed $^{26}\text{Al}/^{10}\text{Be}$ ratios below the constant exposure-erosion island. If the sample is representative of nuclide ratios at the time of deposition of the lower unit, then recycling of previously buried deposits has occurred and the critical assumption of a simple two-stage geomorphic history is invalid. This interpretation is supported by the presence of eroded high-level gravel deposits in the Manzi River headwaters. A reasonable alternative is that the modern alluvial sample is predominantly derived from old Luangwa deposits recently eroded by the Manzi River and does not represent the nuclide inventory of the lower deposits at the time of their deposition. Additional analyses of modern Manzi River and Luangwa River alluvium will be required to choose between the two interpretations.

Accurate ^{10}Be surface exposure dating of the upper portion of the section cannot be performed because of the lack of an exponential nuclide concentration trend. This makes it impossible to compute an exposure age corrected for nuclide inheritance using the method of Anderson et al. (1996). A correction based on modern alluvium of the Manzi River would not be valid because of the apparent difference in sources between the two deposits. An accurate exposure age for surface clasts is also not possible because isotopic evidence for long burial means that an unknown amount of the cosmogenic nuclide inventory produced by former exposure may have been lost to radioactive decay.

In summary, dating of the Manzi section with cosmogenic ^{26}Al and ^{10}Be using either burial dating method was unsuccessful because of uncertainties regarding the exposure history of sediments hosting Mode 1 artefacts and the significance of an unconformity. This finding corrects preliminary age estimates previously released (Phillips et al., 2005; Colton, 2009). At the time of sampling, the sediments of the section were thought to be entirely derived from the relatively small, steep Manzi River catchment. This geometry favours sediment sourcing from a landscape of erosional equilibrium with most nuclide production on steadily eroding hillslopes followed by rapid transport and a single episode of burial. Further geomorphic analysis (Colton, 2009)² and our cosmogenic nuclide data throw doubt on this simple history. In one scenario, deposits of the mainstream Luangwa may have been repeatedly recycled, with multiple episodes of burial and exposure. Although the nuclide ratios of the four deepest samples are consistent with long burial, under these conditions the assumptions of "simple" burial dating do not apply and accurate ages cannot be computed (Balco and Rovey, 2008). In addition, robust surface exposure dates for the upper deposits and surface clasts cannot be computed.

Although the results were disappointing, they contribute to a developing awareness of the complex depositional and erosional

² The cosmogenic nuclide ages reported in Colton (2009) are derived from calculations that assumed the sediments originated from the catchment of the Manzi River. This assumption was incorrect and these published ages are invalid.

history of fluvial sediments in this portion of the Luangwa River basin, and this knowledge can be used to refine archaeological prospection strategies. At least 3.8 m of sediment have been lost above the Manzi section based on our survey from the SF datum to the top of the adjacent hill. Seven kilometres to the northwest of the Manzi section are artefact-bearing gravels with similar typological sequences (Modes 1 and 3), although they are concentrated in 1 m thick deposits that cap a series of concordant hilltops that rise 20 m above the Luangwa floodplain (Colton, 2009). A considerable amount of erosion by incision has evidently taken place, probably in the Pleistocene, to produce the present-day dissected land surface. Geomorphological features indicative of high energy erosional events (landslides, debris slide, and coarse fan deposits) have been reported to the southeast of the Luangwa Valley and attributed to late Quaternary glacial phase aridity (Thomas, 1999). Moore et al. (2007:327) identified an episode of tectonic uplift of the Zambian plateau in the mid-Pleistocene as a major transformational event that altered drainage patterns across the region. The Luangwa Valley would have been affected by the latter. Further geomorphological research supported by numerical dating is needed in the Valley to test the hypothesis of recent uplift and erosion.

Palaeomagnetic sampling

Eight oriented monoliths, 20–30 cm in length and labelled MA to MH, were collected for palaeomagnetic analysis from the finer-grained, clayey sand sediments between cobble layers CL2 to CL6 (Fig. 14). Monolith MA was situated between cobble layers CL2 and CL3 at the bottom of the modern soil layer and consisted of reddish, porous sand. The other monoliths, MB to MH (unaffected by the modern soil development), were collected from the grey clayey sands below cobble layer CL3. Special attention was paid to the

bottom part of the section—two monoliths, ME and MH, were collected from lenses of finer-grained sediment between cobble layers CL5 and CL6, immediately above the layer of broken red mudstones. One additional monolith, MD1, came from immediately above cobble layer CL5.

Seven smaller monoliths, MK1 to MK7, were collected from the red mudstones (tentatively assigned to the Karoo Group) in order to compare their magnetic properties to those of the overlying fluvial deposits. Unorientated (soil) samples were also collected from different depths in the modern soil and bagged, also for comparative magnetic mineral analysis.

In the field, the monoliths were orientated using either a level top or a vertical side surface. Onto this surface a reference direction was determined with respect to magnetic north (using a magnetic compass). The dip direction of this plaster surface was determined to an accuracy of one degree. In order to preserve the sedimentary and palaeomagnetic integrity of these relatively poorly consolidated sediment samples, the monoliths were permeated with sodium silicate solution in the field as well as later in the laboratory. They were then cut into horizontal layers of 2.3 cm thickness, each monolith containing between 6 and 8 such layers (labelled as MA1 to MA7 for monolith MA, as MB1 to MB8 for monolith MB, etc.). Each of these layers in turn yielded between 6 and 20 standard 2.2 cm palaeomagnetic sample cubes. Between one and six of the best preserved and finer-grained specimens from each layer were used in the laboratory palaeomagnetic analysis. Three to four standard cubic specimens were also cut from the Karoo samples.

The palaeomagnetic methods applied to the sampled Manzi specimens include measurements of their natural remanent magnetisation (NRM) and the response of the NRM to various thermal and/or alternating field demagnetisation procedures (as detailed in the SOM). The Koenigsberger factor, the ratio between the NRM and the induced magnetisation in a 0.05 mT field (i.e., approximately Earth's magnetic field intensity), was calculated. This ratio is used as an indication of the nature and stability of the NRM of the specimens.

In addition, the magnetic susceptibility and magnetic remanence acquisition behaviour of the samples were measured in order to characterise the magnetic mineralogy of the sediments (details in SOM).

Magnetic results

Table 5 lists the mean magnetic properties of monoliths MA to MH from the sampled Manzi section. The uppermost monolith, MA, from the weathered, reddish sands, stands out against the underlying grey, finer-grained monoliths (MB–MH), displaying values of NRM and Q_{NRM} ($NRM\ 0.31\ 10^{-5}\ Am^2/kg$ and $Q_{NRM}\ 0.93$) that are two times higher.

Table 5

Mean mass specific magnetic parameters NRM, χ_{LF} , and Q_{NRM} of the fluvial sediments (monoliths MA–MH) and of the underlying red mudstones (samples MK1–MK7)

Group	N_s	NRM ($10^{-5}\ Am^2/kg$)	χ_{LF} ($10^{-8}\ m^3/kg$)	Q_{NRM}
MA	33	0.31	7.9	0.93
MB	36	0.16	7.6	0.53
MG	40	0.08	5.7	0.37
MC	30	0.10	6.8	0.39
MF	38	0.11	5.1	0.56
MD	36	0.09	5.6	0.43
ME	23	0.10	4.5	0.56
MH	24	0.07	6.0	0.30
Red mudstones (Karoo Group)	36	1.62	22.7	1.88

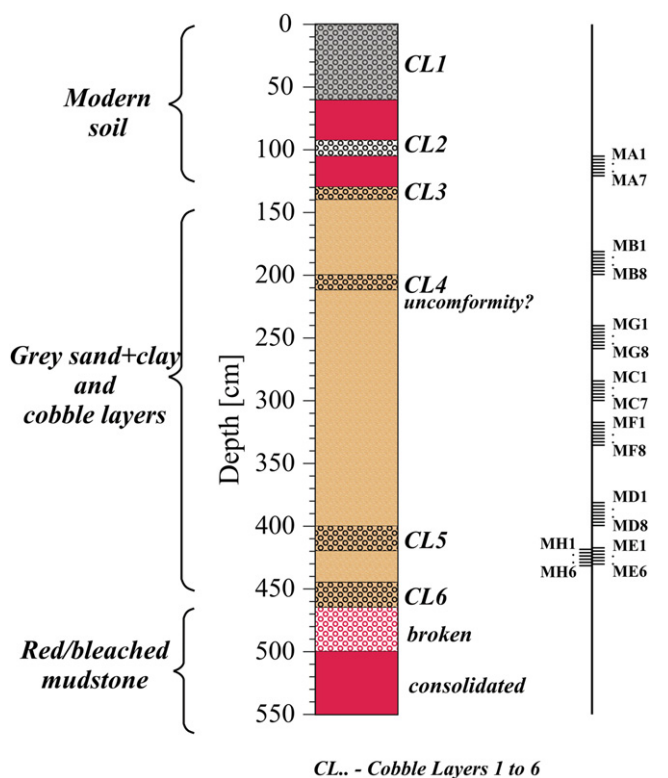


Fig. 14. Schematic diagram showing the positions of the monoliths collected from the sandy parts of the fluvial sediments from the main section (SF), Manzi River.

The same pattern is observed when the saturation remanent magnetisation (SIRM) and the magnetic susceptibility values of representative sedimentary specimens and of powder soil samples are compared (Fig. 15). The SIRM and susceptibility values are four to five times higher in the upper, weathered soil compared to the underlying finer-grained (clayey sand) monoliths MB–MH. It is evident that soil development in the upper 1.3–1.5 m of the section (encompassing the topmost monolith MA) has resulted in enhancement of the magnetic mineral content at this part of the section (Maher, 1998). It is possible that the palaeomagnetic properties of this uppermost part of the section are recent and ‘overprinted’ as a result of this modern soil development.

If we now compare the remaining fluvial part of the sequence with the basal red mudstones (Fig. 16), it can be seen that the fluvial sediments acquire a lower percentage of their SIRM (between 8 and 12%) at high applied fields (in this case, above 300 mT). This indicates that they contain a higher proportion of ‘soft’, ferrimagnetic minerals, like magnetite (or, correspondingly, a lower proportion of the ‘harder’ magnetic mineral, haematite). The values of the ratio of SIRM and magnetic susceptibility are uniformly low throughout the section, varying from 6.9 to 16.2 kA/m (9.84 kA/m on average). Values in this range indicate the absence of any iron sulphide minerals, such as greigite (Hallam and Maher, 1994; Maher and Hallam, 2005).

The natural remanence of the fluvial sediments at Manzi is dominated to varying degrees by weakly magnetic haematite mineral grains of (predominantly) detrital origin. Only trace amounts of the much more strongly magnetic magnetite-like minerals are present, within the finer sediment fractions, where these occur. For much of the sequence, the coarse-grained nature of these sediments has precluded efficient acquisition of a stable depositional remanence. Where the NRM is stable, it may be either

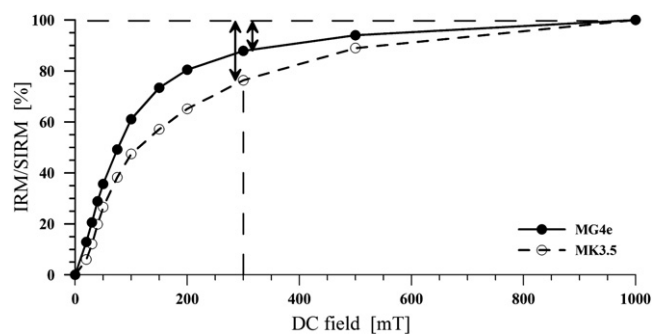


Fig. 16. IRM acquisition in fields up to 1 T for representative fluvial (MG4e, solid line) and basal red mudstone (MK3.5, dashed line) samples. The high-field remanence is typically between 8 and 12% in the fluvial sediments and 20 to 25% in the basal mudstones.

syn- or post-depositional in nature, but is preferentially carried by the trace fraction of ferrimagnetic (magnetite-like) grains within the finer-grained, clayey fraction, where present.

Palaeomagnetic results

The SOM provides the details of the demagnetisation characteristics and the palaeomagnetic polarity classification obtained from the Manzi samples. The sequence displays three distinct sets of palaeomagnetic properties. From the top of the sequence, the strongly magnetic samples from the uppermost monolith MA (1.1–1.3 m beneath the soil surface) consistently yielded normal (N) polarities, suggesting a Brunhes age (i.e., <780 ka) of their NRM. However, the observed enhancement of their magnetic properties, in comparison with the underlying sediments, shows that the MA sediments have been strongly influenced by post-depositional soil development. Under these conditions, their normal magnetisation may either reflect the geomagnetic field at the time of sediment deposition or, conversely, have been acquired as a later ‘overprint’ as magnetite was formed in situ within the soil.

In contrast to these upper sediments, all of the monoliths sampled from below cobbles layer CL3 are uniformly weakly magnetised and record reversed rather than normal magnetic polarity. Their NRM is dominated by weakly magnetic haematite, contained in the sand fraction, with only a trace amount of magnetite-like material, present primarily within the finer size fractions. For dating purposes, palaeomagnetists use various demagnetisation procedures to ‘clean’ the NRM in order to isolate the stable, so-called ‘characteristic remanent magnetisation’ (the ChRM). This stable ChRM is that component of the remanence which most faithfully records the Earth’s magnetic field at the time the sediment was deposited. For the Manzi sediments, stable ChRMs were successfully isolated in approximately 70% of the specimens from the upper part of the section (i.e., from monoliths MA, MB, MG, MC, and MF). These ChRMs were isolated mostly by using alternating field demagnetisation (in the intermediate magnetic stability range, between 10–15 and 30–40 mT). This procedure ‘cleans’ that part of the NRM carried by the trace magnetite-like component. Monoliths MB, MG, MC, and MF (from between 1.8 and 3.4 m beneath the soil surface) all exhibit unambiguously magnetically reversed (R) polarities. In the lower parts of the section, the proportional contribution of haematite to the NRM increases. Hence, the NRM intensity decreases, and the failure rate of the magnetic ‘cleaning’ increases; 50% of the experiments failed to produce identifiable ChRM directions and another 15% are of very poor quality. Notwithstanding this high failure rate, all of those ChRM directions that were retrieved within this section of the sequence are consistently of reversed, Matuyama-like polarity.

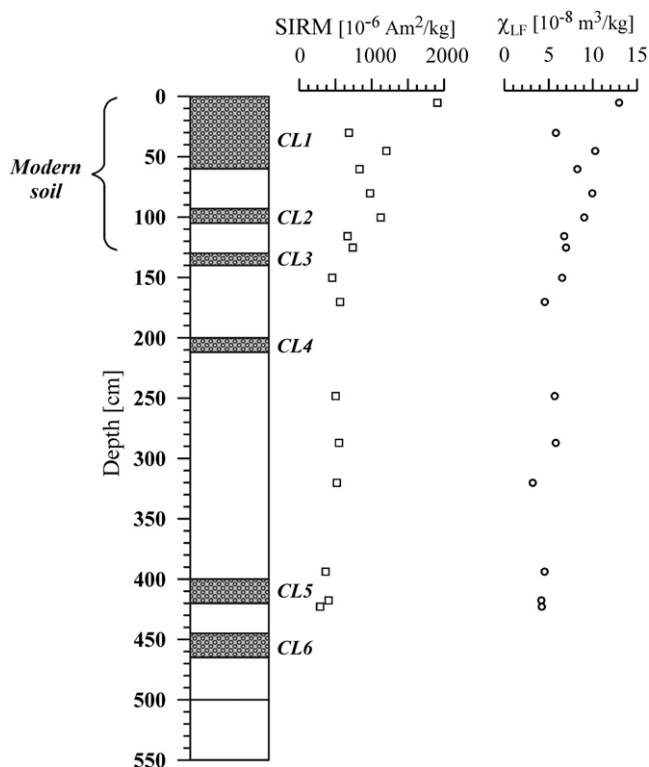


Fig. 15. Combined plot of the saturation IRM and of the magnetic susceptibility of specimens from the underlying fluvial sediments and the uppermost sediment layers affected by modern soil development.

The palaeomagnetic properties of the sediments change again towards the base of the fluvial sequence. The lowermost monoliths, ME and MH (which occupy the same stratigraphic position between cobble layers CL5 and CL6), yielded approximately an equal number of normal and reversed polarity specimens (with 70% of the specimens failing to produce stable ChRMs). Some specimens displayed both reversed and normal polarities in the intermediate coercivity range. Amongst the good quality results, some 75% were of normal polarity.

Figure 17 summarises the palaeomagnetic results and the magnetic polarity sequence interpreted for the sediments. Three magnetozones can readily be distinguished in the Manzi sediments:

1. The sediments from the uppermost monolith MA, situated at 1.1–1.3 m beneath the soil surface (between cobble layers CL2 and CL3), yielded consistently normal polarities, suggesting the NRM is of Brunhes age (i.e., <780 ka). However, the observed enhancement of the magnetic properties in this upper monolith compared with the rest of the section shows that the upper sediments have been strongly affected by the development of secondary ferrimagnetic minerals in the modern soil. The age of their NRM may thus be much younger than the age of the sediment itself.
2. Monoliths MB, MG, MC, and MF, from between 1.8 and 3.4 m beneath the soil surface, exhibit unambiguously reversed polarities. We ascribe these reversed polarities to palaeomagnetic remanence acquisition by the sediments during the Matuyama Chron (i.e., between 2.5 Ma and 780 ka).
3. The lowermost monoliths, ME and MH, which occupy the same stratigraphic position between cobble layers CL5 and CL6, yielded a mixture of both normal and reversed polarity specimens. We have assigned the magnetozone polarity for

ME and MH as predominantly normal on the basis that the normal polarities are observed in more than one good quality specimen per sampling level and in more than one adjacent sampling level. The caveat here is that a number of good-quality reversed polarity specimens are also present. The relatively coarse-grained nature of the sediment at this point in the sequence and the presence of both reversed and normal polarities suggest rapid rates of sediment deposition and slightly varying ages of the blocking-in, or ‘recording’ process, of the NRM, at the time of a normal-to-reversed geomagnetic transition.

Thus, we interpret these mixed polarity directions in the lower 0.30 m of the fluvial section at Manzi (CL5/6) to probably represent sediment deposition at the time of transition from a normal polarity sub-chron into a reversed polarity chron (the Matuyama, from ~2.5–0.78 Ma). The identity and time of this transition could include: the end of the Jaramillo normal sub-chron, at ~0.98 Ma; the Cobb Mountain, at ~1.17 Ma; the Olduvai, at ~1.78 Ma; or the Reunion, at ~2.11 Ma (Hornig et al., 2002).

Isothermal thermoluminescence dating—methods and results

In trench A1, located at the highest point of the Manzi section 9.6 m above the current river level, three sediment samples (Aber87/SL62, 63, and 64) for luminescence dating were collected from the face exposed by excavation (Fig. 18). The samples were collected underneath a black tarpaulin and placed immediately into opaque black plastic bags to exclude daylight. An additional sample (SL61) was collected from the channel of the modern Manzi River as

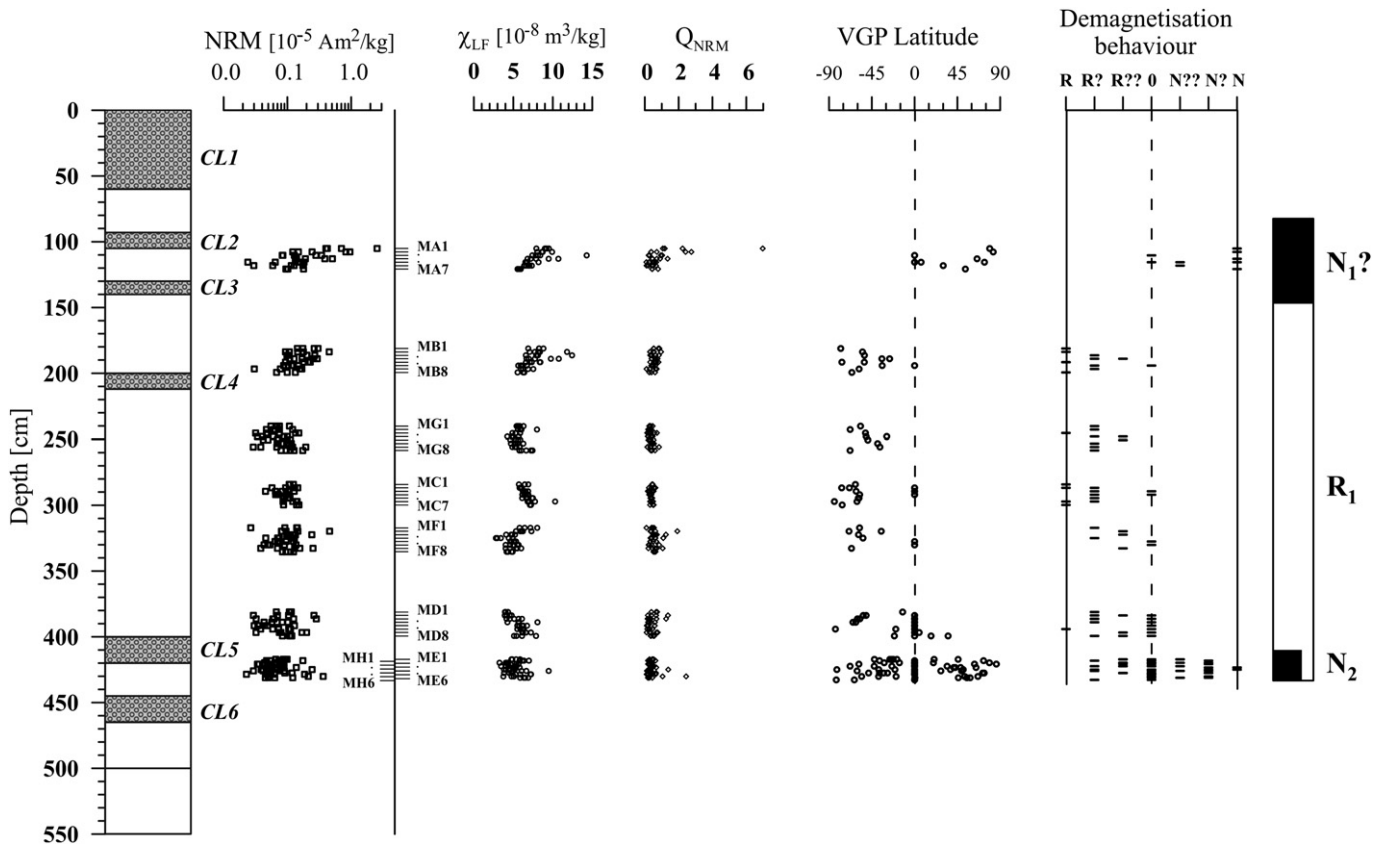


Fig. 17. NRM, magnetic susceptibility, and VGP latitude and demagnetisation behaviour classification of the Manzi section specimens.

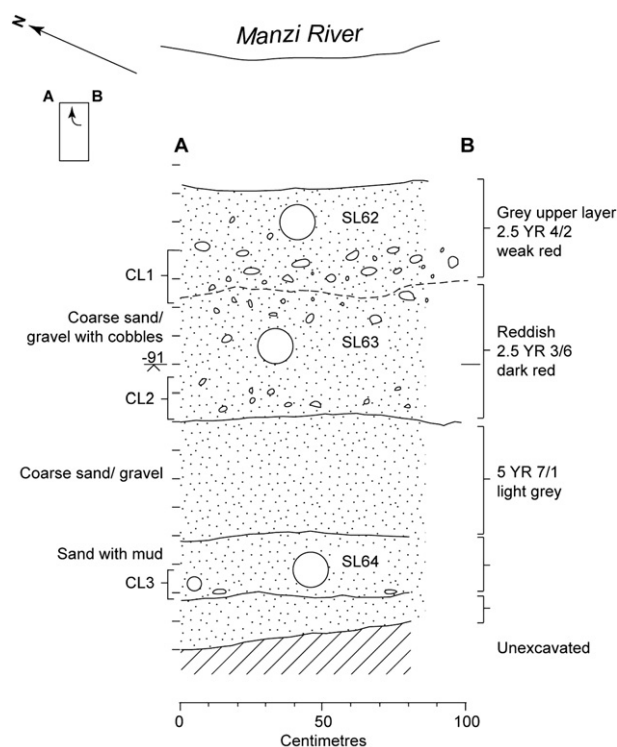


Fig. 18. Unit A1 section showing the location of luminescence samples in relation to cobble layers (CL1–CL3) and the colour boundary between upper red soil and underlying grey sediments.

a modern analogue of the depositional environment of the other samples. Samples Aber87/SL62 and SL63 are stratigraphically equivalent to sediments above and below CL1 in the main section excavation, effectively bracketing this layer. Sample Aber87/SL64 lies above CL3, giving a maximum age for CL2, and is the stratigraphic equivalent of palaeomagnetic monolith MA. The samples represent the uppermost and presumably youngest part of the Manzi sequence.

Equivalent dose determination

Under red safelight conditions in the Aberystwyth Luminescence Research Laboratory, the samples collected for luminescence measurements were treated with H_2O_2 and HCl to remove organic material and carbonates, respectively. Quartz grains were isolated through a combination of density separation, using sodium polytungstate, and etching in concentrated hydrofluoric acid for 40 min.

The fast component of the optically stimulated luminescence (OSL) signal from quartz is well suited to dating sediments because the signal is reduced to a low level by exposure to daylight in a matter of tens of seconds (Godfrey-Smith et al., 1988; Duller, 2004). It is this signal which has been used extensively for dating sediments from archaeological sites and other Quaternary sites, using either multiple grain methods or single grain methods (Jacobs and Roberts, 2007; Duller, 2008). However, initial measurements made on sample Aber87/OS2 which had been collected from the same site at Manzi in 2003 showed that the fast component of the OSL signal was saturated (Jain et al., 2007: Fig. 4a); thus, the sediments were too old to be dated using this signal. Therefore, an alternative method of analysis capable of measuring another luminescence signal, one that is light sensitive but that could also grow to higher radiation doses, was required.

If quartz is heated to 310 °C and then held at that temperature, a luminescence signal is emitted that then decays with time, falling to a low level after 200–500 s. This is called isothermal thermoluminescence (ITL), and this signal continues to grow at radiation doses above that at which the OSL signal is saturated. Since dating with ITL is new and experimental, Jain et al. (2007) undertook a range of experiments on sample Aber87/OS2 to characterise the dose response of the signal and its bleaching characteristics. The dose response curve was measured using a single aliquot regenerative dose (SAR) protocol where all the luminescence measurements are made on a single sub-sample, or aliquot. This type of protocol had been used extensively in luminescence dating (Wintle and Murray, 2006) and is specifically designed to compensate for any changes in luminescence sensitivity that may occur during a sequence of measurements. The growth of the luminescence signal is normally mathematically fitted with a saturating exponential of the form shown in Equation (1).

$$I_D = I_{Max} \times \left[1 - e^{-\left(\frac{D}{D_0}\right)} \right] \quad (1)$$

The rate at which any luminescence signal (I_D) saturates is specified by the parameter D_0 . In their study of the fast component of the OSL signal Wintle and Murray (2006) have suggested that interpolation onto the growth curve becomes prone to errors above doses which are twice the value of D_0 , and this acts as the limit for dating. For the OSL signal from Aber87/OS2 measured using an SAR protocol, the value of D_0 was 50 ± 3 Gy. For the same sample, the ITL signal was also measured using an SAR protocol as described in Jain et al. (2007); this gave a value for D_0 of 440 ± 40 Gy, suggesting that the ITL signal could date events up to nine times older than the OSL. Analysis of the dose response curve for the samples discussed here shows a similar value of D_0 for the ITL signal, with the dose response curve for one disc being shown in Fig. 19.

One disadvantage of the ITL signal is that it is not as light sensitive as the OSL signal. Jain et al. (2007) showed that the ITL signal fell to about 10% of its initial value after 4,000 s of exposure to a SOL 2 solar simulator, a lamp that is six times stronger than direct sunlight. In order to check whether the ITL signal in sediments from the Manzi River are reset in nature by exposure to daylight, sample Aber87/SL61 was collected from 0.25 m below the surface of the modern Manzi channel. Given the intensity of rainfall during wet seasons, this sediment is likely to have been deposited within the previous few years. ITL measurements gave an equivalent dose (D_e) of 15.0 ± 1.0 Gy. For OSL measurements the residual signal in fluvial sediments would typically be much lower than this (Jain et al., 2004); however, the value of 15 Gy obtained from the ITL measurements shows that this signal is sufficiently well reset at deposition to allow the method to be applied to older sediments.

In previous applications of ITL, Jain et al. (2005), Gibling et al. (2005), and Choi et al. (2006) obtained ages on fluvial, loess, and beach sediments that appeared to be consistent with geological expectations. In addition, Choi et al. (2006) were able to successfully recover a range of different laboratory doses, adding to their confidence in the method. However, both Huot et al. (2006) and Buylaert et al. (2006) found that ITL gave overestimates of D_e due to a large and irreversible sensitivity change during the initial measurement of the natural ITL signal at 310 °C; unlike Choi et al. (2006) they were not able to recover a given laboratory dose. Changes of sensitivity during the first ITL measurement are very challenging since the sensitivity of the sample is only measured in the SAR sequence at the end of the first ITL measurement (Jain et al., 2007).

To overcome the sensitivity change during the first ITL measurement, a modified SAR procedure has been developed and is shown in Table 6. This differs from previous methods in the way in

Table 6
Modified SAR procedure used for ITL measurements

Step	Signal measured	
1	Preheat 280 °C for 10 s	
2	Measure ITL at 310 °C for 3 s	L_N
3	Bleach sample in SOL2 for 110 min	
4	Test dose D_i	
5	Preheat 280 °C for 10 s	
6	Measure ITL at 310 °C for 250 s (use first 3 s for analysis of T_N)	T_N
7	Regeneration dose (D_i)	
8	Preheat 280 °C for 10 s	
9	Measure ITL at 310 °C for 250 s (use first 3 s for analysis of L_x)	L_x
10	Test dose D_i	
11	Preheat 280 °C for 10 s	
12	Measure ITL at 310 °C for 250 s (use first 3 s for analysis of T_x)	T_x
13	Repeat steps 7–12 with different regeneration doses	

SOL 2 induced Sensitivity correction procedure		
Regeneration dose (D_i) – repeat point in the same approximate dose range as the D_e		
Preheat 280 °C for 10 s		
Measure ITL at 310 °C for 3 s		L_c
Bleach sample in SOL2 for 110 min		
Test dose D_i		
Preheat 280 °C for 10 s		
Measure ITL at 310 °C for 250 s (use first 3 s for analysis of T_c)		T_c

which the natural ITL signal is measured. Previously the sample had been heated to 310 °C and the ITL signal was measured for up to 500 s. This long period of time at 310 °C is the cause, at least in some samples, of a large change in sensitivity which leads to incorrect D_e values and the inability to recover a known laboratory dose. To avoid this problem in the current study the natural ITL signal was measured only for 3 s at 310 °C and the sample was then cooled. To remove the remaining ITL signal the sample was then bleached in a SOL2 solar simulator for 110 min. Like the ITL measurement for 500 s, the SOL2 bleaching removes the ITL signal, but the critical advantage of the SOL2 approach is that it reduces the magnitude of any sensitivity change due to the thermal treatment during the first measurement; this would ideally make the first measurement of sensitivity (T_N) more appropriate for monitoring the sensitivity of the 3 s ITL measurement of L_N . SOL2 bleaching, however, introduces about 30% sensitivity increase in the subsequent test dose ITL signal due to optical treatment. This change was observed to be only weakly dependent on dose and it was not specific to the natural measurement. The sensitivity change could, therefore, be estimated by measuring one of the repeat (recycle) points (L_c/T_c) lying close to the 'natural' dose in the same manner as the 'natural' cycle (Table 6). Finally the 'natural' signal (L_N/T_N) was corrected for the SOL2 induced sensitivity change for the D_e estimation. The growth of the sensitivity-corrected ITL signal is then constructed using just the first 3 s of the ITL measurements (Fig. 19).

Ideally a new method like this should be tested by comparing the ages obtained with independent dating methods. However, obtaining samples that are both suitable for luminescence dating and have good independent age control beyond the range of radiocarbon is difficult, and none are known that would be directly relevant to this study. The other dating methods applied in this paper provide some constraint on the ITL ages. Another approach to assess whether this procedure was working correctly is to undertake a dose recovery experiment on the modern sample Aber87/

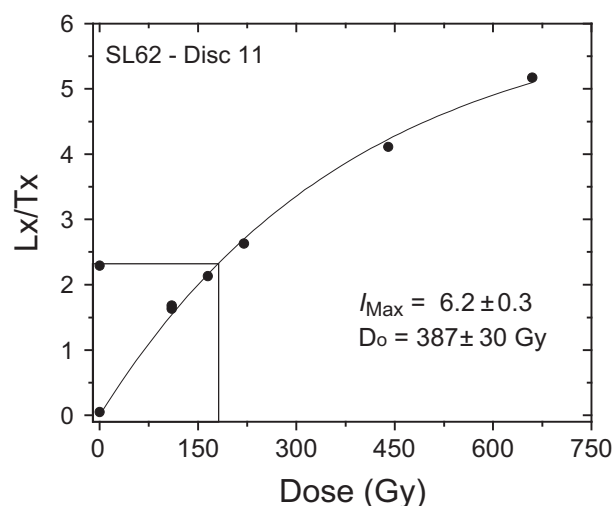


Fig. 19. Sensitivity-corrected dose response curve for the ITL signal from one aliquot of sample Aber87/SL62.

SL61. Nineteen aliquots were given a known laboratory dose of 110 Gy and then measured using the procedure shown in Table 6. The average dose measured was 125 ± 4 Gy. Subtracting the residual dose of 15 ± 1 Gy measured for this sample gave a dose recovery ratio of 1.01 ± 0.03 , demonstrating the ability of the new procedure to recover a dose.

For each of the three samples collected for dating, twelve D_e values were measured using ITL. The typical form of the dose response curve for these aliquots is shown in Fig. 19, demonstrating that the dose giving rise to the natural signal is far below the saturation dose for this signal. In each case the signal resulting from a regeneration dose of 110 Gy was measured twice so that a recycling ratio could be calculated, and these were within the range 0.9–1.1. The distribution of D_e values for each sample is shown in Fig. 20. The cause of the higher scatter for sample Aber87/SL63 is not clear. The mean and standard error of the D_e values were calculated and used for age calculation (Table 7).

Dose rate determination

The dose rate to the samples was assessed through a combination of in situ gamma spectrometry and laboratory beta counting. Because of the coarse nature of the sediment, in situ gamma spectrometry using a 2 inch NaI crystal linked to an Ortec Micro-Nomad system was used to determine the gamma dose rate to each of the samples. The limited range of beta particles means that the beta dose will predominantly come from the fine sand-sized material between the clasts. The beta dose rate from these sands was measured in the laboratory using a GM-25-5 beta counter, analysing finely milled sub-samples of the material collected for luminescence measurement. The current depth of the samples below the ground surface are 0.30 (SL62), 0.63 (SL63), and 1.40 m (SL64). The lowering of the immediate local land surface by approximately 4 m as estimated from our survey results means the cosmic dose rate to the samples will have changed through time. For calculation of the cosmic dose rate, 0.5 m have been added to the excavation depths shown in Table 7 and an uncertainty of 0.5 m was included in the calculation. At these sites the cosmic dose rate only contributes 4.8–6.8% of the total dose rate, so uncertainty in this value has a small impact on the final ages.

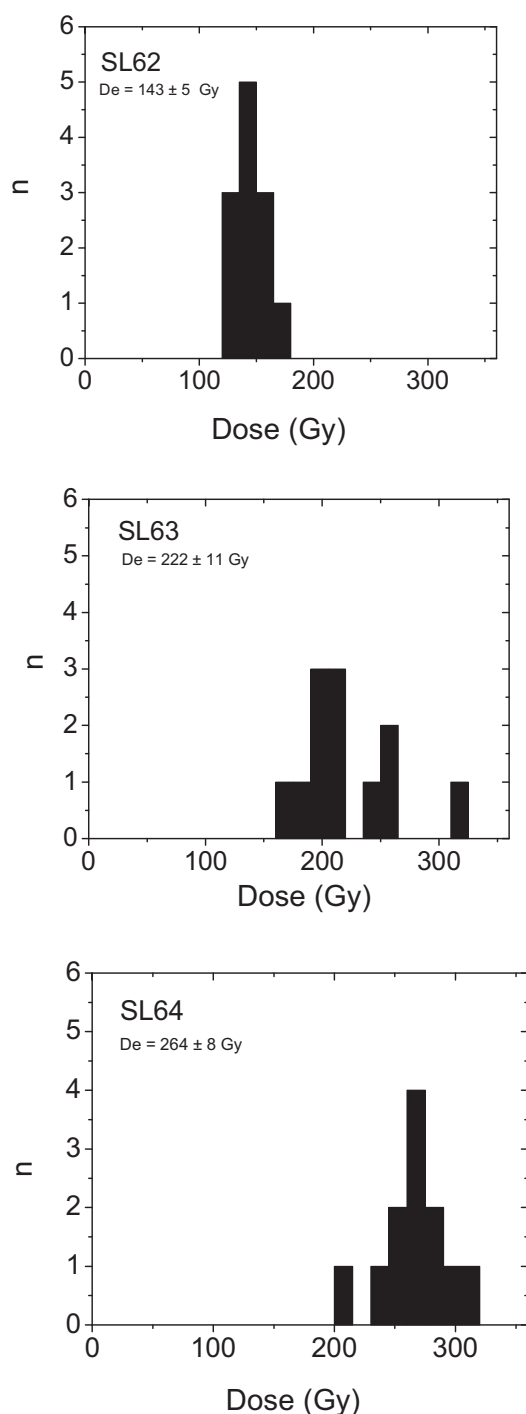


Fig. 20. Distribution of D_e values for each of the three samples analysed. The mean and standard deviation of the D_e from the 12 aliquots measured for each sample is also given.

Interpretation of ITL ages

The ITL dose response curves measured for the three samples (e.g., Fig. 19) demonstrate that the natural ITL signal is not close to the limit of saturation. The ability to recover a dose using the new SAR protocol described in Table 6 adds to the confidence in the D_e values obtained. The ages obtained are listed in Table 7, along with the dosimetry data. The ages for the lower two samples (Aber87/SL63 and SL64) are indistinguishable within the uncertainties, while the uppermost sample (SL62) gives a much younger age (36.4 ± 2.1 ka).

We could interpret these results two ways. First, that all the ages are recording the depositional age of the unit from which they were collected. The uppermost sediment is 36 ka, and the two lower samples are essentially the same age. Combining the ages for the lower two samples gives a best estimate of 78.1 ± 5.0 ka. This interpretation implies that it has taken 40,000 years to deposit 30 cm of sediment, or that erosion has occurred. It also implies that there was still deposition on this surface as recently as 36 ka.

Alternatively, we could interpret things differently. The uppermost luminescence sample (SL62) was collected very close to the modern ground surface (0.3 m). It is conceivable that this age is not the depositional age as this surface is essentially a lag deposit due to winnowing of fines from the ground surface. This process may have also introduced some more recent fine material which has become mixed with the existing sediment (which is perhaps only slightly younger than 74 ka), thus giving an age that is much younger than 74 ka. In this scenario the upper age does not really tell us anything useful, and the best estimate we have is that all the sediments in the upper 1.3 m of Trench A1 were deposited 78.1 ± 5.0 ka (the average of the two lower ages), and that at some time after that the Manzi river incised below the level of this terrace; sediment deposition then ceased and slow lowering of the ground surface began.

Interpreting the age of the Manzi sequence and its archaeological implications

The upper unit Mode 3 cobble layers CL1 and CL2 are late Pleistocene in age and probably date to ~78 ka based on the averaged ITL ranges for CL2. CL1 in this interpretation is treated as an unreliable sample and removed from further consideration. If CL1 does indicate a later period of sedimentation then the uppermost deposit has a more complex history with a gap in deposition between CL1 and CL2 of at least 30,000 years. The normal Brunhes chron polarity of the deposit represented by monolith MA adds some very general support to the age estimates of these uppermost deposits and their archaeological content. Unfortunately, the small artefact sample hampers further culture-stratigraphic discussion beyond a generic Mode 3 classification and its known age range in south-central Africa. Intermittent Mode 3 occupation is recorded at the site of Mumbwa Caves in central Zambia with assemblages dated to MIS5e, d, and MIS3 with the site abandoned during the later phases of MIS 5 through to MIS3 (between ~90–40 ka; Barham, 2000:41). The Luangwa Valley may have been a refuge for hunter-gatherer populations during arid glacials and stadials

Table 7
Sampling and analytical data for the three samples collected from Trench A1 for dating using ITL

Sample code (Aber87)	Sample depth (m)	Grain size (μm)	Beta dose rate (Gy/ka) ^a	Gamma dose rate (Gy/ka) ^a	Cosmic dose rate (Gy/ka)	Total dose rate (Gy/ka)	D_e (Gy)	Age (ka)
SL62	0.30 ± 0.10	90–150	3.04 ± 0.18	0.70 ± 0.04	0.19 ± 0.05	3.93 ± 0.19	143 ± 5	36.4 ± 2.1
SL63	0.63 ± 0.10	90–150	1.83 ± 0.12	0.62 ± 0.03	0.18 ± 0.05	2.63 ± 0.14	215 ± 11	81.6 ± 5.9
SL64	1.40 ± 0.10	90–150	2.23 ± 0.13	1.15 ± 0.06	0.17 ± 0.04	3.54 ± 0.15	264 ± 8	74.5 ± 3.9

^a A water content of $20 \pm 5\%$ has been used in calculating the dose rate due to the high seasonal rainfall in the area.

(Barham, 2000:227), and perhaps the dates from the Manzi are signalling a continuing human presence in the Valley late into MIS5 when other areas of south-central Africa were depopulated as a consequence of reduced or unreliable rainfall (Scholz et al., 2007). A substantially more refined database for the Luangwa Valley is needed to develop and test these speculative correlations between climate change and population movements.

The age of CL3 remains unknown, but the palaeomagnetic record brackets this cobble layer between the Brunhes normal chron (monolith MA) and the Matuyama reversed chron (monolith MB). A significant temporal or depositional hiatus may separate CL3 from CL2, but this is purely speculative in the absence of a numerical age for CL3. The artefact sample from CL3 is also too small to generate a relative chronology based on technological change within this Mode 3 sequence.

The unsuccessful attempt to model the cosmogenic burial age of the lower unit (CL4–CL6) leaves the polarity of the deposits as the only guide to the likely age range of the artefacts. The presence of a Mode 1 strategy for producing flakes is an uncertain chronological marker given the longevity of this technology. There are currently no numerically dated Mode 1 sites in south-central Africa to provide a chronological benchmark for the region. Mode 1 Oldowan assemblages in East Africa range in age from 2.6 to ~1.7 Ma and in South Africa are estimated to be 2.0–1.7 Ma (Kuman, 1998). The age of Mode 1 assemblages in the Luangwa Valley should logically fall between the eastern and southern African range given the geographical position of the Luangwa Valley and assuming a southerly spread of hominins using this technology. If the Manzi's lower unit is attributable to the Oldowan, then the deposit is likely to be early Pleistocene in origin. A range of possible palaeomagnetic matches is possible given the transitional normal polarity at the base of CL6: the deposit could indeed be as recent as 0.98 Ma (i.e., the normal-to-reversed transition at the end of the Jaramillo) or 1.17 Ma (end of the Cobb Mountain). The Mode 1 artefacts in this case would be too young to be attributed with confidence to the Oldowan industry given its known age range (2.6–1.7 Ma). Three alternative interpretations are offered to explain this potential discrepancy between the technology and its potential sub-chron associations.

First, the artefacts are indeed Oldowan but occur in much younger re-deposited contexts. The heavy abrasion on much of the CL5 assemblage supports this option, but the underlying CL6 material is much less altered with the minimally abraded pieces indicating little transport. Alternatively, the artefacts reflect an essentially Mode 2 variant in which bifaces were absent. The continuing use of Mode 1 flake technology in the Acheulean of eastern Africa and western Asia is well known (e.g., Gowlett, 1988; Bar-Yosef and Goren-Inbar, 1993; Potts et al., 1999; Schick and Clark, 2003; Delanges et al., 2006; Tryon and Potts, 2006), and the rarity of bifaces generally in the Luangwa Valley makes it difficult to distinguish between Modes 1 and 2 on the basis of flakes and cores alone. In this instance, the attribution to Mode 2 is made on the basis of negative evidence. Large flake size (>10 cm) may be indicative of a conceptually Mode 2 technology that emphasises long, continuous cutting edges (Clark, 2001b), but in the case of the lower unit the flake length rarely exceeds 4 cm (Table 3). A third possibility merits consideration assuming a date of ~1 Ma for the lower unit: Mode 1 remained the dominant technology in the Luangwa Valley long after its replacement elsewhere in Africa. The Valley does support endemic sub-species of zebra (*Equus burchellii crawshaii*), wildebeest (*Connochaetes taurinus cooksoni*), and giraffe (*Giraffa camelopardalis thornicrofti*), and by analogy perhaps hominins in the Valley retained an effective flake technology as a response to local restrictions on raw material size and form. Bifaces do occur sporadically in this mid-portion of the Luangwa

Valley, made either by façonnage or débitage depending on the availability of quartzite slabs or cobbles, respectively, but they are rare compared with well-resourced mid-Pleistocene Mode 2 sites such as Kalambo Falls (Clark, 2001a), Isimila (Cole and Kleindienst, 1974), and Olorgesailie (Potts et al., 1999).

In the Luangwa Valley, the distinction between Mode 1 and 2 will remain ambiguous until a site of unequivocal Mode 2 attribution is excavated and dated. The most parsimonious and conservative option, and the one preferred here, is that the lower unit artefacts are no older than 1 Ma and reflect a local response to raw material constraints. The artefacts are technologically Mode 1 but unlikely to be Oldowan in the generally understood sense of the industry as the earliest tool-making tradition (Braun and Harris, 2009). In the absence of other dating evidence, the basal Manzi material cannot be placed with confidence in either the basal transitional normal polarity at the onset of the Olduvai (~1.78 Ma) or Reunion (~2.11 Ma) sub-chrons.

Although the burial age for the lower unit could not be determined at this site, cosmogenic nuclide dating remains the only numerical dating method currently available that spans the Quaternary and which can be applied to otherwise undateable fluvial contexts typical of much of the continent outside the Rift Valley. Electron spin resonance dating of single quartz grains holds promise for extending chronologies to ~2 Ma (Beerten and Stesmans, 2005, 2006), but the approach is still experimental and untested in African archaeological contexts. With the development of numerical dating control of fluvial deposits generally, Palaeolithic archaeologists are now reassessing the behavioural and palaeoenvironmental potential of river terraces for making inter-regional comparisons (Mishra et al., 2007). For the Luangwa Valley, the Manzi excavations represent the first tentative steps towards developing a local independent chronological framework for the Stone Age record and for understanding the relatively recent geomorphological processes that have sculpted the Valley. Considerably more sites will need to be identified and treated to this process of crosschecking using independent lines of dating evidence. This will take time, but the application and refinement of new dating techniques is essential for the development of continental-scale perspectives on regional variability in hominin behavioural and anatomical evolution. The unique geological conditions which led to the formation and preservation of the Rift Valley sequences will ensure that they retain their primacy, but in time research in other lesser known regions, such as the Luangwa Valley, will bring greater geographical and chronological balance to the long African record.

Acknowledgements

We thank the anonymous referees and Daryl Granger for their critical comments which helped us reassess our initial cosmogenic results. Any remaining errors are ours entirely. We also thank the Zambia Wildlife Authority (ZAWA) and the National Heritage Conservation Commission (NHCC) for their support in the field and for granting permission for this research. Funding for the excavations and dating analyses (cosmogenic and palaeomagnetic) was provided by the Arts and Humanities Research Council (AHRC), UK, as part of the Luangwa Valley Past Peoples and Environments Project. The ITL dating was funded by the EFCHED scheme of the Natural Environment Research Council (NERC), UK. A special thank you is given to Evonne Beadnell for the fine artefact illustrations.

Appendix. SOM

Supplementary data associated with this article can be found in the online version, at doi:10.1016/j.jhevol.2010.12.003.

References

- Anderson, R.S., Repka, J.L., Dick, G.S., 1996. Explicit treatment of inheritance in dating depositional surfaces using in situ Be-10 and Al-26. *Geology* 24, 47–51.
- Andrews, B.N., 2006. Sediment consolidation and archaeological site formation. *Geoarchaeology* 21, 461–478.
- Astle, W.L., 1971. Management in the Luangwa Valley. *Oryx* 11, 135–139.
- Balco, G., Rovey, C.W., 2008. An isochron method for cosmogenic-nuclide dating of buried soils and sediments. *Am. J. Sci.* 308, 1083–1114.
- Barham, L., 1987. The bipolar technique in southern Africa: a replication experiment. *S. Afr. Archaeol. Bull.* 42, 45–50.
- Barham, L., 2000. The Middle Stone Age of Zambia, South Central Africa. Western Academic and Specialist Press, Bristol.
- Barham, L., Mitchell, P., 2008. The First Africans: African Archaeology from Earliest Tool-makers to Most Recent Foragers. Cambridge University Press, Cambridge.
- Bar-Yosef, O., Goren-Inbar, N., 1993. The Lithic Assemblages of Ubeidiya: a Lower Palaeolithic Site in the Jordan Valley. The Hebrew University of Jerusalem, Jerusalem.
- Beaumont, P.B., Vogel, J.C., 2006. On a timescale for the past million years of human history in central South Africa. *S. Afr. J. Sci.* 102, 217–228.
- Beerten, L., Stesmans, A., 2005. Single quartz grain electron spin resonance (ESR) dating of a contemporary desert surface deposit, Eastern Desert. *Egypt. Quatern. Sci. Rev.* 24, 223–231.
- Beerten, L., Stesmans, A., 2006. The use of Ti centers for estimating burial doses of single quartz grains: a case study from an aeolian deposit ~2 Ma old. *Radiat. Meas.* 41, 418–424.
- Bierman, P.R., Gillespie, A.R., Caffee, M.W., 1995. Cosmogenic ages for earthquake recurrence intervals and debris flow fan deposition, Owens-Valley, California. *Science* 270, 447–450.
- Bierman, P.R., Caffee, M.W., Davis, P.T., Marsella, K., Pavich, M., Colgan, P., Mickelson, D., Larsen, J., 2002. Rates and timing of earth surface processes from in situ-produced cosmogenic Be-10. *Beryllium: Mineralogy, Petrol. Geochem.* 50, 147–205.
- Bishop, L., Barham, L., Ditchfield, P., Elton, S., Ohman, J.C., in prep. Fossil fauna from the Luangwa Valley, Zambia: provenance and interpretation.
- Braun, D., Harris, J.W.K., 2009. Plio-Pleistocene technological variation: a view from the KBS Mbr., Koobi Fora formation. In: Schick, K., Toth, N. (Eds.), *The Cutting Edge: New Approaches to the Archaeology of Human Origins*. Stone Age Institute Press, Gosport (Indiana), pp. 17–32.
- Brunet, M., Beauvilain, A., Coppens, Y., Heintz, E., Moutaye, A.H.E., Pilbeam, D., 1995. The first australopithecine 2500 kilometres west from the Rift Valley (Chad). *Nature* 378, 273–275.
- Brunet, M., Guy, F., Pilbeam, D., Mackaye, H., Likius, A., Ahounta, D., Beauvilain, A., Blondel, C., Bocherons, H., Boisseries, J.-R., de Bonis, L., Coppens, Y., Dejax, J., Denys, C., Düringer, P., Eisenmann, V., Fanone, G., Fronty, P., Geraads, D., Lehman, T., Lihoreau, F., Louchar, A., Mahamat, A., Merceron, G., Mouchelin, G., Otero, O., Campomanes, P., Ponce de Leon, M., Rage, J.-C., Sapanet, M., 2002. A new hominid from the Upper Miocene of Chad, Central Africa. *Nature* 418, 145–151.
- Buylaert, J.P., Murray, A.S., Huot, S., Vriend, M.G.A., Vandenberghe, D., De Corte, F., Van den haute, P., 2006. A comparison of quartz OSL and isothermal TL measurements on Chinese loess. *Radiat. Protect. Dosimetry* 119, 474–478.
- Chazan, M., Ron, H., Matmon, A., Porat, N., Goldberg, P., Yates, R., Avery, M., Sumner, A., Horwitz, L.K., 2008. Radiometric dating of the Earlier Stone Age sequence in excavation I at Wonderwerk Cave, South Africa: preliminary results. *J. Hum. Evol.* 55, 1–11.
- Choi, J.H., Murray, A.S., Cheong, C.S., Hong, D.G., Chang, H.W., 2006. Estimation of equivalent dose using quartz isothermal TL and the SAR procedure. *Quatern. Geochronol.* 1, 101–108.
- Clark, J.D., 1954. Upper Sangoan industries from northern Nyasaland and the Luangwa Valley: a case of environmental differentiation? *S. Afr. J. Sci.* 50 (8), 201–208.
- Clark, J.D., 1974. Kalambo Falls Prehistoric Site Volume II: The Late Prehistoric Remains. Cambridge University Press, Cambridge.
- Clark, J.D., 2001a. Kalambo Falls Prehistoric Site Volume III. Cambridge University Press, Cambridge.
- Clark, J.D., 2001b. Variability in primary and secondary technologies of the Later Acheulian in Africa. In: Milliken, S., Cook, J. (Eds.), *A Very Remote Period Indeed: Papers on the Palaeolithic Presented to Derek Roe*. Oxbow Books, Oxford, pp. 1–18.
- Clark, J.G.D., 1969. *World Prehistory: a New Outline*. Cambridge University Press, Cambridge.
- Cole, G.H., Kleindienst, M.R., 1974. Further reflections on the Isimila Acheulian. *Quatern. Res.* 4, 346–355.
- Colton, D., 2009. An archaeological and geomorphological survey of the Luangwa Valley, Zambia. *British Archaeological Reports S2022*, Cambridge Monographs in African Archaeology 78, Oxford.
- Cotterell, B., Kamminga, J., 1979. The mechanics of flaking. In: Hayden, B. (Ed.), *Lithic Use-wear Analysis*. Academic Press, London, pp. 97–112.
- Delanges, A., Roche, H., 2005. Late Pliocene hominid knapping skills: the case of Lokalalei 2C, West Turkana, Kenya. *J. Hum. Evol.* 48, 435–472.
- Delanges, A., Lenoble, A., Harmand, S., Brugal, J.-P., Prat, S., Tiercelin, J.-J., Roche, H., 2006. Interpreting pachyderm single carcass sites in the African lower and early middle Pleistocene record: a multidisciplinary approach to the site of Nadung'a 4 (Kenya). *J. Anthropol. Archaeol.* 25, 448–465.
- Dixey, F., 1937. The geology of part of the upper Luangwa Valley, North-eastern Rhodesia. *Q. J. Geol. Soc.* 93, 52–76.
- Drysdall, A.R., Weller, R.K., 1966. Karoo sedimentation in Northern Rhodesia. *Trans. Geol. Soc. S. Afr.* LXIX, 39–69.
- Duller, G.A.T., 2004. Luminescence dating of Quaternary sediments: recent advances. *J. Quatern. Sci.* 19, 183–192.
- Duller, G.A.T., 2008. Single grain optical dating of Quaternary sediments: why aliquot size matters in luminescence dating. *Boreas* 37, 589–612.
- East, R., 1984. Rainfall, soil nutrient status and biomass of large African savanna mammals. *Afr. J. Ecol.* 22, 245–270.
- Elton, S., Barham, L., Andrews, P., Sambrook Smith, G.H., 2003. Pliocene femur of *Theropithecus* from the Luangwa Valley, Zambia. *J. Hum. Evol.* 44, 133–139.
- Gathogo, P.N., Brown, F.H., 2006. Revised stratigraphy of Area 123, Koobi Fora, Kenya, and new age estimates of its fossil mammals, including hominins. *J. Hum. Evol.* 51, 471–479.
- Gibson, R., Granger, D., Kuman, K., Partridge, T., 2009. Early Acheulean technology in the Rietputs formation, South Africa, date with cosmogenic nuclides. *J. Hum. Evol.* 56, 152–160.
- Gibling, M.R., Tandon, S.K., Sinha, R., Jain, M., 2005. Discontinuity-bounded alluvial sequences of the southern Gangetic Plains, India: aggradation and degradation in response to monsoonal strength. *J. Sediment. Res.* 75, 369–385.
- Gillespie, J.D., Tupakka, S., Cluney, C., 2004. Distinguishing between naturally and culturally flaked cobbles: a test case from Alberta, Canada. *Geoarchaeology* 19, 615–633.
- Gilvear, D., Winterbottom, S., Sickingabula, H., 2000. Character of channel planform change and meander development: Luangwa River, Zambia. *Earth Surf. Process. Landforms* 25, 421–436.
- Godfrey-Smith, D.I., Huntley, D.J., Chen, W.H., 1988. Optical dating studies of quartz and feldspar sediment extracts. *Quatern. Sci. Rev.* 7, 373–380.
- Gowlett, J.A.J., 1986. Culture and conceptualisation: the Oldowan-Acheulean gradient. In: Bailey, G.N., Callow, P. (Eds.), *Stone Age Prehistory: Studies in Memory of Charles McBurney*. Cambridge University Press, Cambridge, pp. 243–260.
- Gowlett, J.A.J., 1988. A case of developed Oldowan in the Acheulean? *World Archaeol.* 20, 13–26.
- Granger, D.E., Smith, A.L., 2000. Dating alluvial sediments using radioactive decay and muogenic production of ²⁶Al and ¹⁰Be. *Nucl. Instrum. Methods Phys. Res. B.* 172, 822–826.
- Granger, D.E., Muzikar, P.F., 2001. Dating sediment burial with in situ-produced cosmogenic nuclides: theory, techniques, and limitations. *Earth Planet. Sci. Lett.* 188, 269–281.
- Hallam, D.F., Maher, B.A., 1994. A record of reversed polarity carried by the iron sulphide, greigite in British early Pleistocene sediments. *Earth Planet. Sci. Lett.* 121, 71–80.
- Hanks, T.C., Finkel, R.C., 2005. Early Pleistocene incision of the San Juan River, Utah, dated with ²⁶Al and ¹⁰Be: Comment and Reply: COMMENT. *Geology* 33, e78–e79. doi:10.1130/0091-7613-33.1.e78.
- Hornig, C.-S., Lee, M.-Y., Pålke, H., Wei, K.-Y., Liang, W.-T., Lizuka, Y., Torrii, M., 2002. Astronomically calibrated ages for geomagnetic reversals within the Matuyama chron. *Earth Planet. Space* 54 (6), 679–690.
- Huot, S., Buylaert, J.P., Murray, A.S., 2006. Isothermal thermoluminescence signals from quartz. *Radiat. Meas.* 41, 796–802.
- Intera Information Technologies, Ltd. (ITT), 1992. Petroleum potential of the Luangwa Valley, 1992. Unpublished report filed in the Geology Department, Government House, Lusaka.
- Jacobs, Z., Roberts, R.G., 2007. Advances in optically stimulated luminescence (OSL) dating of individual grains of quartz from archaeological deposits. *Evol. Anthropol.* 16, 210–223.
- Jain, M., Murray, A.S., Bøtter-Jensen, L., 2004. Optically stimulated luminescence dating: how significant is incomplete light exposure in fluvial environments. *Quaternaire* 15, 143–157.
- Jain, M., Bøtter-Jensen, L., Murray, A.S., Denby, P.M., Tsukamoto, S., Gibling, M.R., 2005. Revisiting TL: dose measurement beyond the OSL range using SAR. *Ancient TL* 23, 9–24.
- Jain, M., Duller, G.A.T., Wintle, A.G., 2007. Dose response, thermal stability and optical bleaching of the 310 °C isothermal TL signal in quartz. *Radiat. Meas.* 42, 1285–1293.
- Kubik, P.W., Ivy-Ochs, S., Masarik, J., Frank, M., Schluchter, C., 1998. Be-10 and Al-26 production rates deduced from an instantaneous event within the dendro-calibration curve, the landslide of Kofels, Oetz Valley, Austria. *Earth Planet. Sci. Lett.* 161, 231–241.
- Kuman, K., 1998. The earliest South African industries. In: Petraglia, M., Korisettar, R. (Eds.), *Early Human Behaviour in Global Context: The Rise of Diversity of the Lower Palaeolithic Record*. Routledge Press, London, pp. 151–186.
- Lebatard, A.-E., Bourlès, D.L., Düringer, P., Jolivet, M., Braucher, R., Carcaillet, J., Schuster, M., Arnaud, N., Monié, P., Lihoreau, F., Likius, A., Mackaye, H.T., Vignaud, P., Brunet, M., 2008. Cosmogenic nuclide dating of *Sahelanthropus tchadensis* and *Australopithecus bahrelghazali*: Mio-Pliocene hominids from Chad. *Proc. Natl. Acad. Sci.* 105, 3226–3231.
- Macrae, F.B., Lancaster, D.G., 1937. Stone Age sites in Northern Rhodesia. *Man* XXXVII, article 74.
- Maher, B.A., Hallam, D.F., 2005. Magnetic carriers and remanence mechanisms in magnetite-poor sediments of Pleistocene age, southern North Sea margin: paper II. *J. Quatern. Sci.* 20, 79–94.

- Maher, B.A., 1998. Magnetic properties of modern soils and loessic paleosols: implications for paleoclimate. *Palaeogeogr. Palaeoclimatol. Palaeoecol.* 137, 25–54.
- Mishra, S., White, M.J., Beaumont, P., Antoine, P., Bridgland, D.R., Limondin-Lozouet, N., Santisteban, J.L., Schreve, D.C., Shaw, A.D., Wenban-Smith, F.F., Westaway, R.W.C., White, T.S., 2007. Fluvial deposits as an archive of early human activity. *Quatern. Sci. Rev.* 26, 2996–3016.
- Moore, A.E., Cotterill, F.P.D., Main, M.P.L., Williams, H.B., 2007. The Zambezi River. In: Gupta, A. (Ed.), *Large Rivers: Geomorphology and Management*. John Wiley and Sons, London, pp. 311–332.
- Newcomer, M.H., 1971. Some quantitative experiments in handaxe manufacture. *World Archaeol.* 3 (1), 85–94.
- Partridge, T.C., 2000. Hominid-bearing cave and tufa deposits. In: Partridge, T.C., Maud, R.R. (Eds.), *The Cenozoic of Southern Africa*. Oxford University Press, New York, pp. 100–129.
- Partridge, T.C., Granger, D.E., Caffee, M.W., Clarke, R.J., 2003. Lower Pliocene hominid remains from Sterkfontein. *Science* 300, 607–612.
- Pavlish, L.A., Kleindienst, M.R., Sheppard, P.J., 2002. Flume experiments with stone and bone. In: Jerem, E., Biró, K.T. (Eds.), *Archaeometry 98*. Archaeopress BAR S1043, Oxford, pp. 613–620.
- Phillips, W.M., Barham, L.S., Kubik, P.W., 2005. Dating alluvial sediments with cosmogenic nuclides. *Geochim. Cosmochim. Acta* 69, A166.
- Phillips, W.M., McDonald, E.V., Reneau, S.L., Poths, J., 1998. Dating soils and alluvium with cosmogenic Ne-21 depth profiles: case studies from the Pajarito Plateau, New Mexico, USA. *Earth Planet. Sci. Lett.* 160, 209–223.
- Plummer, T., 2004. Flaked stones and old bones: biological and cultural evolution at the dawn of technology. *Yearb. Phys. Anthropol.* 47, 11–164.
- Potts, R., 2001. Mid-Pleistocene environmental change and human evolution. In: Barham, L.S., Robson-Brown, K. (Eds.), *Human Roots: Africa and Asia in the Middle Pleistocene*. Western Academic & Specialist Press, Bristol, pp. 5–21.
- Potts, R., Behrensmeier, A.K., Ditchfield, P., 1999. Paleolandscape variation and early Pleistocene hominid activities: members 1 and 7, Olorgesailie formation, Kenya. *J. Hum. Evol.* 37, 747–788.
- Sahnouni, M., Hadjouis, D., van der Made, J., Derradji, A.-El-K., Canals, A., Medig, M., Belahrech, H., Harichane, Z., Rabhi, M., 2002. Further research at the Oldowan site of Ain Hanech, North-eastern Algeria. *J. Hum. Evol.* 43, 925–937.
- Schick, K., Clark, J.D., 2003. Biface technological development and variability in the Acheulean industrial complex in the middle Awash region of the Afar Rift, Ethiopia. In: Sorressi, M., Dibble, H.L. (Eds.), *Multiple Approaches to the Study of Bifacial Technologies*. University Museum Monograph 115, Philadelphia, pp. 1–30.
- Schnurrenberger, D., Bryan, A.L., 1985. A contribution to the study of the nature/artifact controversy. In: Plew, M.G., Woods, J.C., Pavesic, M.G. (Eds.), *Stone Tool Analysis: Essays in Honor of Don E. Crabtree*. University of New Mexico Press, Albuquerque, pp. 133–159.
- Shackley, M., 1978. The behaviour of artefacts as sedimentary particles in a fluvial environment. *Archaeometry* 20, 55–61.
- Sharon, G., Beaumont, P., 2006. Victoria West – a highly standardised prepared core technology. In: Goren-Inbar, N., Sharon, G. (Eds.), *Axe Age: Acheulian Tool-making from Quarry to Discard*. Equinox, London, pp. 181–199.
- Sheppard, P.J., Kleindienst, M., 1996. Technological change in the earlier and middle Stone Age of Kalambo Falls (Zambia). *Afr. Archaeol. Rev.* 13, 171–196.
- Scholz, C.A., Johnson, T.C., Cohen, A.S., King, J.W., Peck, J.A., Overpeck, J.T., Talbot, M.R., Brown, E.T., Kalindekafu, L., Amoako, P.Y.O., Lyons, R.P., Shanahan, T.M., Castañeda, I.S., Heil, C.W., Forman, S.L., McHargue, L.R., Beuning, K.R., Gomez, J., Pierson, J., 2007. East African megadroughts between 135 and 75 thousand years ago and bearing on early-modern human origins. *Proc. Natl. Acad. Sci.* 104, 16416–16421.
- Thomas, M.F., 1999. Evidence of high energy landforming events on the central African plateau: eastern Zambia. *Z. Geomorph.* 43, 273–297.
- Toth, N., 1985. The Oldowan reassessed: a close look at early stone artifacts. *J. Archaeol. Sci.* 12, 101–120.
- Trapnell, C.G., 1996. *The Soils, Vegetation and Traditional Agriculture of Zambia, Volume II: North Eastern Zambia Ecological Survey 1937–1942*. Redcliffe Press, Bristol.
- Trauth, M.H., Maslin, M.A., Deino, A.L., Strecker, M.R., Bergner, A.G.N., Dühnforth, M., 2007. High- and low-latitude forcing of Plio-Pleistocene East African climate and human evolution. *J. Hum. Evol.* 53, 475–486.
- Tryon, C.A., McBrearty, S., 2006. Tephrostratigraphy of the Bedd Tuff Member (Kaphurin Formation, Kenya) and the nature of archaeological change in the later middle Pleistocene. *Quatern. Res.* 65, 492–507.
- Tryon, C.A., Potts, R., 2006. Approaches for understanding flake production in the African Acheulian. Paper submitted to the Electronic Symposium “Core Reduction, Chaîne Opératoire, and Other Methods: The Epistemologies of Different Approaches to Lithic Analysis” at the 71st Annual Meeting of the Society for American Archaeology, San Juan, Puerto Rico, April 2006 (accessed online 3.12.06).
- Utting, J., 1988. An introduction to the geological history of the South Luangwa National Park, Zambia. Geological Survey Department, Special Publication, Lusaka.
- Vail, J.R., 1969. The southern extension of the East African rift system and related igneous activity. *Int. J. Earth Sci.* 57, 601–614.
- Walker, J., Cliff, R.A., Latham, A.G., 2006. U–Pb isotopic age of the Stw 573 hominid from Sterkfontein, South Africa. *Science* 314, 1592–1594.
- Wenban-Smith, F.F., Allen, P., Bates, M.R., Parfitt, S.A., Preece, R.C., Stewart, J.R., Turner, C., Whittaker, J.E., 2006. The Clactonian elephant butchery site at Southfleet Road, Ebbsfleet, UK. *J. Quatern. Sci.* 5, 471–483.
- Williams, F.L., Ackermann, R.R., Leigh, S.R., 2007. Inferring Plio-Pleistocene southern African biochronology from facial affinities in *Parapapio* and other fossil papionins. *Am. J. Phys. Anthropol.* 132, 163–174.
- Wintle, A.G., Murray, A.S., 2006. A review of quartz optically stimulated luminescence characteristics and their relevance in single-aliquot regeneration dating protocols. *Radiat. Meas.* 41, 369–391.
- Wolkowinsky, A.J., Granger, D.E., 2004. Early Pleistocene incision of the San Juan River, Utah, dated with Al-26 and Be-10. *Geology* 32, 749–752.